THE ABSOLUTE QUANTUM EFFICIENCY OF CALCIUM TUNGSTATE WITH LEAD IN THE EXTREME ULTRAVIOLET REGION

by

Virendra Nath Saxena

Principal Investigator: Dr. William A. Rense

UNIVERSITY OF COLORADO
Laboratory for Atmospheric and Space Physics
Boulder, Colorado 80302

SCIENTIFIC REPORT NO. 1

NASA Grant No. NGR 06-003-034

Period Covered: 1 February 1965 - 30 June 1966

NATIONAL AERONAUTICS AND SPACE ADMINISTRATION
WASHINGTON 25, D. C.

TABLE OF CONTENTS

CHAPTER		PAGE
I.	INTRODUCTION	1
II.	A BRIEF DESCRIPTION OF THE APPARATUS	20
	The Vacuum Spectrograph	20
	The Schueler Source	20
	The Source Control Cabinet	23
	The Power Supply	26
	Densitometer Photometer and Accessories . .	26
	Thermopile Accessories	28
	The Phosphor Sample Holder	34
	The Photometer	34
III.	THE ANALYSIS OF THE DATA	38
IV.	CONCLUSION	56
BIBLIOGRAPHY	. . . . .	59
APPENDIX.	THE THEORETICAL VALUES OF R	62

LIST OF FIGURES

FIGURE		PAGE
1 (a,b,c)	Insulator, Semiconductor, Metal	6
2	Klasen's Model (Electron capture)	8
3	Lambe's Model (Hole capture)	9
4	Configuration Coordinate Diagram	11
5.(a,b)	Radiation transfer in crystals	14
6a	Relative Response Curves, linear	16
b	Relative Response Curves, Semi-log	17
7	Lambert's Law	18
8	Vacuum Monochromator	21
9	Schueler Source	22
10	Gas Metering System	24
11	Source Control Cabinet	25
12	Power Supply	27
13	Thermopile Amplifier and Recorder	29
14 (a,b)	Sample & Thermopile in position behind slit .	30
15	Photometer Mechanical Arrangement	31
16	Optical v's Areal Density Curves	33
17	Photometer Response & Phosphor Emission Curves	40
18	$\omega_{2eff}/\omega_{1eff}$ - Illustration	42
19	Relative Response v's β Graph at 304 A . . .	47
20	Relative Response v's β Graph at 461 A . . .	49
21	Relative Response v's β Graph at 584 A . . .	51
22	Relative Response v's β Graph at 1048 A . . .	53
23	Relative Response v's β Graph at 1216 A . . .	55

LIST OF TABLES

TABLE		PAGE
1.	Optical Density of Phosphor	32
2.	Relative Emission of $CaWO_4$:Pb	41
3.	Values of Constants	45
4.	Summary of Data at 304 A	46
5.	Summary of Data at 461 A	48
6.	Summary of Data at 584 A	50
7.	Summary of Data at 1048 A	52
8.	Summary of Data at 1216 A	54

35236

ABSTRACT

This report discusses the results of the application of a method developed by Bruner[6] for measuring the absolute quantum efficiency of a luminescent material, a quantity which is important from both theoretical and practical viewpoints. This type of research has several applications in the UV spectroscopy of upper air and space physics.

Lead is shown to be an activator for the phosphorescence of calcium tungstate (although pure crystals of this alkaline earth tungstate also exhibit luminescence). In this work the absolute quantum efficiency of $CaWO_4$ with 0.70% lead by weight was measured at room temperature at five selected UV wavelengths. A Reeder thermopile made of gold and blackened with evaporated colloidal gold, and a specially constructed RCA 931 A photomultiplier type photometer were used to measure the intensity of the incident UV radiation and the luminescent radiation coming out from the back of a thin phosphor screen, respectively. The calibration of the photometer was accomplished with the help of the thermopile such that the final results were independent of the absolute sensitivity of either instrument. Appropriate corrections for the absorption and scattering of light within the sample have been made. The Schueler lamp and a one meter grazing incident vacuum monochromator with a 600 lines/mm blazed grating provided spectral lines with enough energy for dependable measurements with the thermopile between 304 A and 1216 A.

The absolute quantum efficiency of the phosphor was found to be of the order of 4.95 at 304 A, 3.53 at 461 A, 3.02 at 584 A, 1.49 at 1048 A and 1.47 at 1216 A, i.e., decreasing with increasing wavelengths in the extreme ultraviolet. There was a suggestion of the possibility of the efficiency attaining a constant value for wavelengths greater than 1000 A. The importance of the results has been discussed in the light of present knowledge of the luminescence phenomena as applied to the inorganic phosphors.

CHAPTER I

INTRODUCTION

The term "luminescence" or cold light was first used in 1888 by Weidmann,[1] for all those phenomena of light which are not solely conditioned by the rise in temperature. The emission of light from matter in the visible or near ultraviolet region under the influence of an exciting agent is termed "fluorescence." The emission of radiation is characteristic of the emitting substance, and to some extent, of the exciting agent. When the emission of the visible light persists after removal of the exciting agent, the process is termed "phosphorescence" or after-glow. The dividing line between the two phenomena is set at a persistence time of nearly 10^{-8} sec, the typical age of an excited state which can cascade down to the lower energy states via an allowed optical transition.

Both phenomena are practically identical and may be explained more or less on the same basis. Luminescence is actually the conventional term covering both, although photoluminescence (by visible light), thermoluminescence (by low heat), triboluminescence (by friction), cathodoluminescence (by cathode rays), sonoluminescence (by sount), chemiluminescence (by chemical reactions), and electroluminescence (by electricity), etc., can also be included. In other words, "luminescence" is classified according to the exciting agent(s) and special prefixes are derived therefrom. Fluorescence may be affected by purity, partical size, age, water content, etc. Although luminescence is also observed in gases and liquids, most of the research effort in this field of study is confined to solids and especially to crystals commonly know as "phosphors."

The phosphor research has many applications, both theoretical and experimental in UV spectroscopy of the upper atmosphere and celestial bodies (phosphors have been used as wavelengths converters), and in the development of cathode ray screens, fluorescent lamps, and scintillation counters. What is most important to the UV spectroscopists is the use of phosphors for the sensitizing and calibration of photographic films and phototubes.

The investigation to be discussed in this report involves the application of a method developed by Bruner[6] for measuring the absolute quantum efficiency of a phosphor by excitation in the extreme UV spectral region. The quantum efficiency is defined as the ratio of the number of the visible photons produced by the exciting UV photons, to the number of ultraviolet photons in the exciting radiation which are absorbed.

When a luminescent crystal absorbs some ultraviolet photons, its electrons are raised from the ground state to several upper excited states. There are many routes along which the excited electrons cascade down to the ground state; giving up their acquired energy. Some of the routes eventually give rise to a few visible photons while others involve only radiationless transitions. A fractional value of the absolute quantum efficiency is indicative of the fact that the so called radiationless transitions are, to some extent, dominate. On the other hand, it is also possible that the absolute quantum efficiency may turn out to be greater than one. When this is the case, it is possible that a very high energy photon, while being absorbed, may release a photoelectron which could, in turn, excite a second electron in the course of donating its kinetic energy. In this way, two electrons may be available to jump to the ground state, and thus, two photons could be ejected. Incidentally, a single photon of say, wavelength 304 A has enough energy to produce as many as sixteen 5000 A photons. Consequently, to observe a quantum efficiency greater than unity is not surprising.

Recent investigation of the upper atmosphere has revived considerable interest in vacuum UV radiation, particularly with respect to the intensity of solar UV which induces various photochemical processes. In 1953, Watanabe and Inn[2] in their studies of excitation spectra, presented a graph of quantum efficiency (not the absolute value) as a function of the incident wavelength of several phosphors in the range 584 A - 3500 A. One of the materials (sodium-salicylate) exhibited the remarkable property that its quantum efficiency was constant over the entire wavelength range. This led many workers to use sodum-salicylate as a reference to which other phosphors were compared.

The previous work of Thurnau[3] and Conklin[12] involved the study of the emission spectra and quantum efficiency of several phosphors relative to sodium-salicylate. In 1964, Samson[4] has shown that the relative quantum

efficiency of sodium-salicylate remains constant between 400 A - 900 A. Recently, Seyas[5] showed that of all the thicknesses of the layer of sodium-salicylate, the one with a weight density of 1.0mg/cm^2 has best response to the 2537 A line of Hg.

Recent work of Bruner[6] on the absolute quantum efficiency of sodium-salicylate shows that the efficiency does not remain constant; rather, it decreases with increasing wavelength varying from 80% to 42% at room temperature between 304 A - 1216 A. Also, the fact that sodium-salicylate exhibits an aging effect[7] was confirmed by Bruner.[6] It was shown by Taylor[8] that crystals of pure calcium-tungstate comprise a very efficient phosphor having about eight times the efficiency of sodium-salicylate. Previously (1933), Swindells[9] had indicated that Pb (lead) acts as an activator for the phosphorescence of calcium and strontium tungstates.

For the purpose of finding the absolute quantum efficiency of a few phosphors, with the absorption and scattering of the UV and visible photons by the crystal and the substrate, and the responsivities of the measuring instruments both taken into account, the present work was begun with available equipment. The first choice of phosphors was an organic phosphor "leumogen,"[10] known to have constant quantum yield. The second was quinine Sulphate.[11] In both cases the response was poor and escaped experimental detection.

However, $CaWO_4$:Pb (common nomenclature for host: activator) gave measureable results. This compound, purchased from General Electric Company of U.S.A. had 0.7% of lead by weight. The excitation spectra of this phosphor had been given by Conklin.[12] Also, the compound is soluble in iso-propyl alcohol and thus produced no difficulty during deposition on the glass substrate.

Before proceeding with the measurement, let us discuss some of the current mechanisms thought to be very important in luminescnece. An exhaustive treatment is given in the literature[13,14,15] on the subject. Since much of the literature reporting research in this field concerns matters closely related to commercial applications, some of the earlier publications appear in commercial reports.[16,17] However, the book of

Leverenz[13] contains a complete account of the luminescence of solids. The books of Kittel[18] and Dekker[19] can also be considered as fairly good references.

In order to explain optical phenomena, mainly luminescence, in non-metallic crystals, one has to have a fair background of the band structure of the electronic energy levels. By the introduction of small traces of impurity, the extra energy levels, which are loaded to the already existing band structure of a crystal, are significant in the understanding of the luminescence behavior. Such pruposeful impurities are called "activators" and the crystal itself is known as "host." An impurity which increases the absorption of some exciting radiation is often called the "sensitizer."

Let us now review, briefly of course, the band theory of solids as it is related to the luminescence process. The free electron model of metals (electron gas) gives us a good deal of insight into several of the physical properties of metals, yet this does not help us understand why some chemical elements crystallize to form good conductors of electricity, while others form insulators, still others form semi-conductors with electrical properties varying with temperature.

We encounter some quite remarkable properties possessed by electrons in crystals when we extend the free electron model to take account of interaction of electrons with the periodic lattice of the solid. We see that the electrons respond to applied electric or magnetic fields as if they are endowed with an effective mass which may be larger or smaller than the free electron mass, or may even be negative. Further, there are situations in which it is convenient to attribute to the charge carriers in crystals a (positive) charge +e; such carriers are known as "holes," in contrast to electrons which behave with their normal (negative) charge -e. The most striking experimental evidence leading to the introduction of the concept of positive current carries or holes in crystal is furnished by the Hall effect.[20] It has been established by means of cyclotron resonance experiments[21] with circularly polarized radiation that holes and electrons rotate in opposite senses in a magnetic field, just as one would expect for charges of opposite sign.

Gragg reflection of "electron waves" is an important and characteristic feature of wave propagation in periodic lattice. For our discussion, the most significant consequence of this is the existence of an energy "gap" in the distribution in energy of the states of the conduction electrons; that is to say there may arise a substantial region of energy in which solutions of the wave equations do not exist. Such energy gaps, or "forbidden energy bands," as they are called, are of decisive nature in determining whether a solid is to be an "insultor" or a "conductor." It will be an insulator if all the energy levels below a forbidden band are filled with electrons and all levels above the forbidden band are vacant and far away, energy-wise, from the filled band. A solid containing an upper energy band which is incompletely filled should have a metallic character. (Figure 1a, 1b, 1c).

It will be evident that the situation depicted above occurs ideally only at absolute zero, when the crystal is in its lowest energy state. At temperatures different from zero, some electrons from the upper filled bands may be excited into the next empty band (conduction band) and concuction becomes possible. If the forbidden energy gap is of the order of several electron volts, however, the solid will remain an "insulator" for all practical purposes. An example is diamond for which the forbidden gap is 7 ev. For a small gap width, say about 1 ev, the number of thermally excited electrons may become appreciable and in this case one speaks of an intrinsic semi-conductor. Examples are germanium and silicon. The distinction between insulators and intrinsic semi-conductors is only a quantitative one. In fact, all intrinsic semi-conductors are insulators at $T = 0$.

By virtue of the low representation of the impurity (producing localized "imperfections" and discreet energy levels) in a host crystal the energy levels therefrom are not densely populated. In fact, the energy levels are relatively far spaced and so there is not too much probability for perturbation which occurs due to the overlapping of their wave functions. An excited electron-hole pair traveling through a crystal is called an "exciton." When an incident photon impinges on a crystal (which is photoconducting), an exciton is produced. The hole and the electron migrate separately. A visible photon, however, is then emitted sometime during the

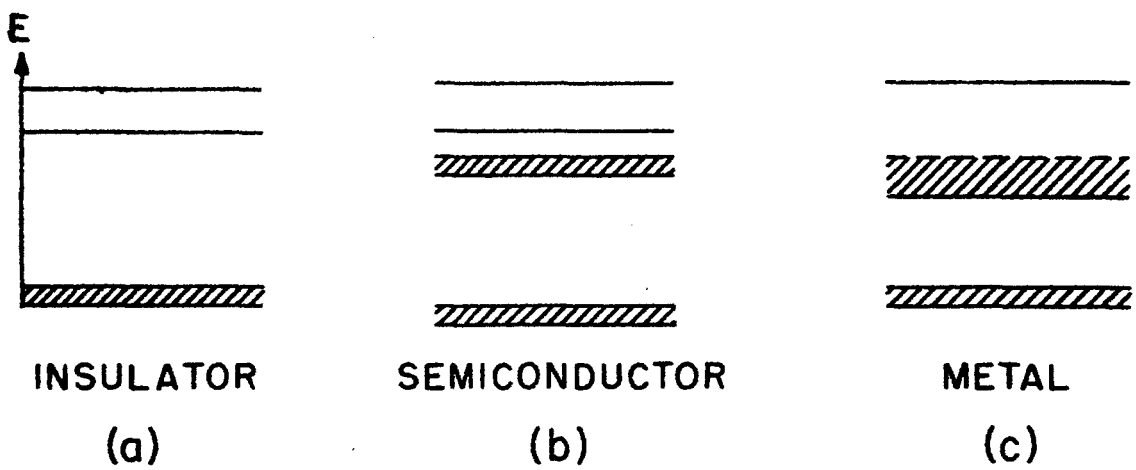

Figure 1

process of recombination. In a non-photoconducting phosphor, absorption of an incident photon excites an electron energy level of one of the activator sites and the return of the electron to the ground state results in the emission of a photon. In either case, the frequency of the emitted photon is lower than the exciting photon.

Typical of the photoconducting phosphor is the family of metal activated zinc and cadmium sulphide compounds; such as, ZnS:Cu, ZnS:Ag and CdS:Ag. Klasens[22] and his associates[23] have proposed a "hole migration" theory of liminescence of sulphides activated with monovalent impurities such as Ag^{+}. The sequence of events is illustrated in Figure 2.

On the ionic picture of the center, the substitution of a monovalent positive ion (Ag^{+}) for a divalent one (Zn^{++}) leaves the volume around the center with a net negative charge. This has two effects: First, the cross section for trapping of a hole becomes large because of coulomb attraction, and second, the energy released in the capture of a hole may be large. The proposed cycle is as below:

(1) Light is absorbed in the fundamental absorption band producing a free electron hole, leading to photoconductivity.

(2) The hole may migrate in the valence band toward the impurity center.

(3) The hole is captured by the impurity center giving off a small amount of energy as infrared or vibrational quanta (Phonon).

(4) The electron wanders through the lattice until it finally comes near the center.

(5) The electron is captured by the center, and gives off excess energy as luminescent emission. The electronic transition may be directly from the conduction band to the ground state of the center or may be by way of an intermediate excited state. After luminescence the cycle is complete and the process may be repeated.

One very striking fact is that the decay of luminescence is much more rapid than the decay of photoconductivity. Since in step 5 above, the decay times of both would be approximately alike, Lambe and Klick[24] suggested a better model given in Figure 3.

In step (3) in this model the hole is captured by the impurigy center and luminescent emission occurs, leaving the center now neutral in

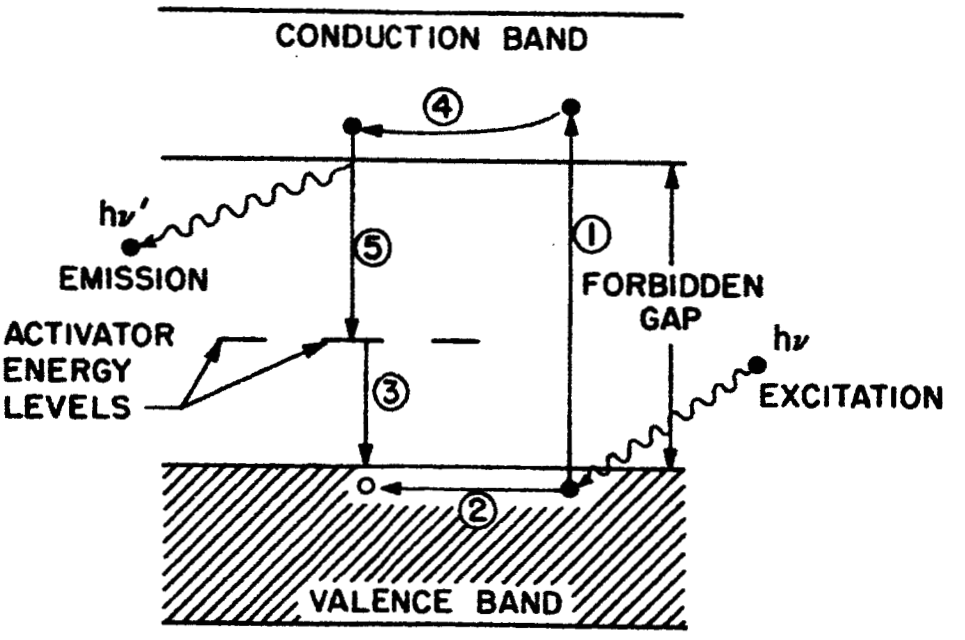

Figure 2.

(1) Excitation, (2) Hole Migration, (3) Hole Capture (non-radiative), (4) Electron Migration, (5) Electron capture resulting in luminescence.

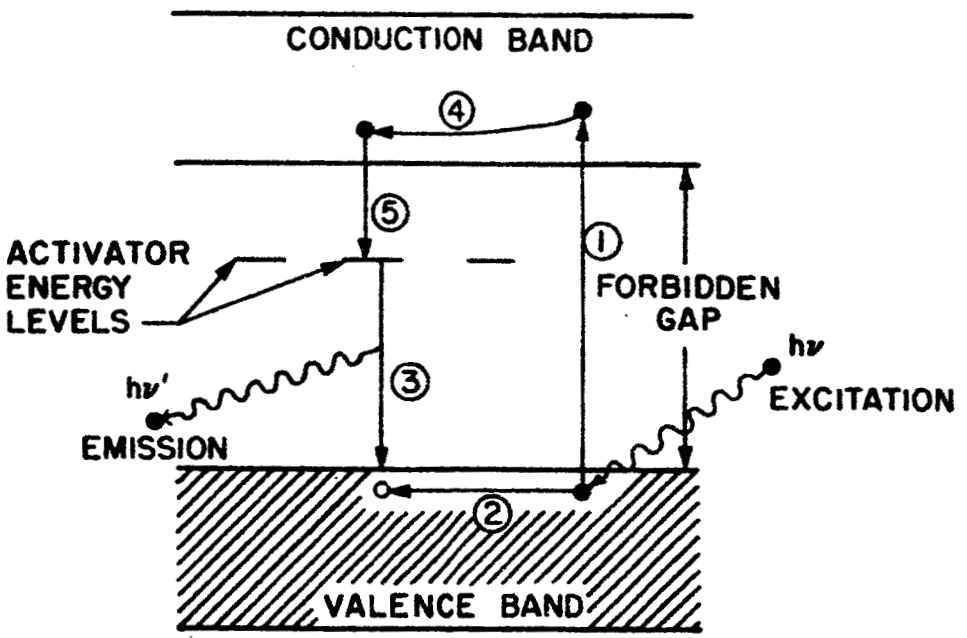
CONDUCTION BAND
④
⑤
①
ACTIVATOR
ENERGY
LEVELS
FORBIDDEN
GAP
hν
hν'
③
EXCITATION
EMISSION
②
VALENCE BAND

Figure 3.

charge; and in step (5) the electron captures a small amount of energy which is given off as an infrared photon or a phonon. The former model assumes that the luminescence results from capture and subsequent recombination of a conduction electron, whereas the latter assumes that it results from the capture and recombination of a free hole.

In this model the luminescent act occurs first and should occur much more rapidly than the decay of photoconductivity. The hole sees an attracting coulomb potential before capture by the activator, while the electron sees a repulsive potential from the activator before the hole is captured and a weak (neutral) potential thereafter. It is known from the independent photoconductivity experiments, that holes are trapped in the sulphides much more rapidly than electrons. The photocurrent is known to be dominated by electrons. Neither silver nor copper in ZnS make the crystal paramagnetic[25] in the ground state, consistent with the Ag^+ assignment of valancy.

The thallium activated alkali halide phosphors have been studied extensively by Williams[26] and provide good example of the class of non-photoconducting phosphors. Thallium ions Tl^+ are believed to occupy the place of K^+ ions. The thallium introduces two bell shaped absorption bands centered about 1960 and 2490 A. The host crystal lattice produces perturbation of the activator energy levels. We shall find it convenient to introduce a potential energy graph (like the Frank-Condon principle in molecular spectroscopy) called the "configuration coordinate diagram." The abscissa represents any single dimensional quantity characterizing the multi-dimensional crystal. In a way, the abscissa depicts the degree of distortion of the lattice.

A typical potential energy vs. configuration sketch is drawn in Figure 4. To illustrate the use of such a Configuration Coordinate diagram, let us consider a simple excitation-emission process. Suppose a crystal originally in its ground state absorbs a near UV photon, raising an electron to a higher orbit and thereby the crystal to an excited state. According to the Frank-Condon principle in molecular spectroscopy, the transition line shown by (1) is vertical because such electron transition takes place in a time short as compared to the lattice vibration period.

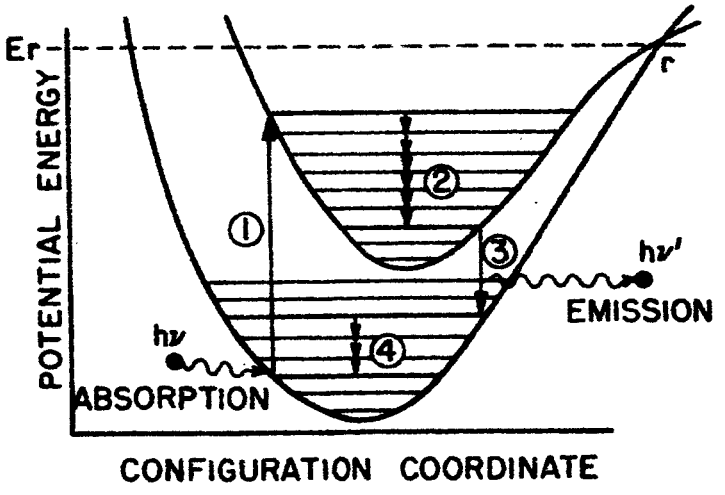
Er
r
POTENTIAL ENERGY
①
②
③
④
hν
ABSORPTION
hν'
EMISSION
CONFIGURATION COORDINATE

Figure 4.

The typical lifetime of the excited states is 10^{-8} sec and the period of lattice vibration is of the order of 10^{-12} sec, therefore, there is considerable time at the disposal of the activator center to come into thermal equilibrium with the lattice. The crystal is now in a non-equilibrium configuration, with considerable thermal motion. This excess energy is dissipated as phonons (Step 2) and the system moves to a lower vibrational level, and the configuration coordinate changes until the equilibrium configuration for the excited state is reached.

The excited electron then returns to the ground state, with the emission of luminescence radiation (Step 3) which shows the emission of a photon of less energy and hence longer wavelength. The final step, denoted by 4, is the thermal dissipation of excess vibrational energy in the form of phonons as the system drops back to its lowest vibrational level

The configuration coordinate diagram proves to be very useful in dealing with the depandence of luminescence phenomena with temperature. If the temperature is high enough and the center receives ample thermal energy to reach the Er level, then the electron has a high probability of jumping to the ground state with no change in energy, i.e., completely radiationless transition. The excess energy is given to the lattice in the form of heat. The vibration level "Er" is a function of temperature and therefore, the luminescence phenomena will be temperature dependent.

Williams[26] has calculated the configuration coordinate curves and predicted the transitions of emission and absorption using approximate wave functions in the case of KCl:Tl, and assuming that the exciting photon was absorbed directly by the activator center. There are other processes where the absorption is due to some other impurity, called a sensitizer, which is introduced in order to enhance absorption outside the activator band. In this case the energy transfer is said to be due to a quantum mechanical resonance phenomena which can occur if the activator and sensitizer wave functions overlap.[27]

Let us now derive, in short, an expression for the absolute quantum efficiency ϵ, taking into account also the self absorption of the luminescent radiation by the phosphor and the substrate. The details are

shown in the report by Bruner.[6] However, only the relevant equations are given here. Consider the figures 5a, 5b in which the phosphor screen of thickness T has been illuminated by the UV radiation of J_o photons/cm^2/sec. Using Bougues law[29] and the initial boundary conditions, one gets:

$$J = J_o e^{-Kx} \quad , \tag{4-2}$$

where K is the constant of proportionality related to the absorption coefficient in the UV.

There are few more assumptions in the remaining steps. Firstly, all the incident UV photons are assumed to be absorbed at the place of impact. This is very true at or near normal incidence.[30,31] Secondly, the emission of the luminescent visible light is supposed to occur at the same place where the exciting UV photon hits it. The tiny crystals of the phosphor produce spherical waves, and correlating this with the fact that the observations are made in the direction of the photometer, that Bougues law holds in the visible also with a different absorption coefficient K', and that the integration is to be accomplished over the entire thickness, T, we obtain finally:

$$I = \frac{\tau\epsilon}{4\pi} J_o \frac{K}{K-K'} \left[e^{-K'T} - e^{-KT}\right] \quad , \tag{4-7}$$

where ϵ is the absolute quantum efficiency, I is the total intensity in photons/cm^2/sec, and τ is the transmission coefficient of the substrate in the visible region.

With a view to study the curves showing the grownth of luminescent radiation with thickness, Bruner[6] defines a new parameter, the "response function," R (K,K',T) :

$$R(K,K',T) = \frac{4\pi I}{\tau\epsilon J_o} = \frac{K}{K-K'} \left[e^{-K'T} - e^{-KT}\right] \quad . \tag{4-8}$$

After defining two other quantities, $\beta = KT$ and $\gamma = K/K'$, we have:

$$R(\beta,\gamma) = \frac{\gamma}{\gamma-1} \left[e^{-\beta} - e^{-\gamma\beta}\right] \quad . \tag{4-11}$$

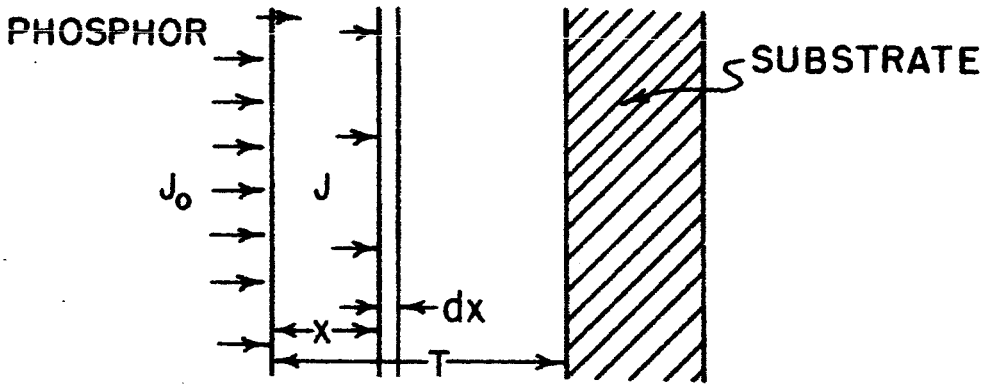

Figure 5 (a).

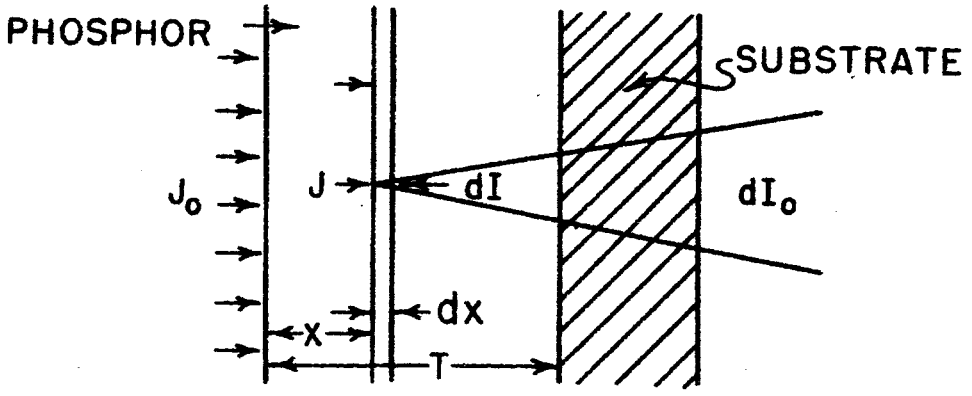

Figure 5 (b).

Now for various values of γ (see appendix A), the theoretical curves between R and β can be drawn.

The transmission coefficient of the phosphor sample τ' in terms of T is devined as $\tau' = e^{-K'T}$. The optical density

$$D = \text{Log}_{10}\frac{1}{\tau'} = \beta \text{ Log}_{10}e \quad , \text{ so that:}$$

$$\beta = \frac{D}{\text{Log}_{10}e} \quad .$$

The curves between R and β have been shown in figures 6a and 6b on linear and semilog scales. They are representative of many physical phenomena as discussed in detail by Bruner[6]. The thickness parameter was found from an optical vs. areal density graph (described later on), and, in order to fix the value of γ, the experimental and theoretical curves on the same scale were matched.

The photometric equation expressing response in terms of certain constants is given by Bruner[6] as:

$$C_p = A_p \, \omega_{eff} \int I(\lambda) \, S_p(\lambda) \, d\lambda \quad , \qquad (4\text{-}15)$$

where $I \, A_p \, \omega_{eff}$ is the total flux entering into the aperture, A_p (see Figure 7) and S_p is the responsivity of the photometer. The integration has been carried out over the intervals of wavelength $d\lambda$, because the luminescent radiation is not monochromatic.

The thermopile response equation is also reproduced below from Bruner's report:[6]

$$C_T = J_o \, A_T, \mu \frac{hc}{\lambda} S_T \quad . \qquad (4\text{-}16)$$

The equations dealing with the inter-calibration part in this experiment are as below:

$$C_{Tc} = I_c \, A_T \, \omega'_{eff} \mu_c \frac{hc}{\lambda_c} S_T \qquad (4\text{-}21)$$

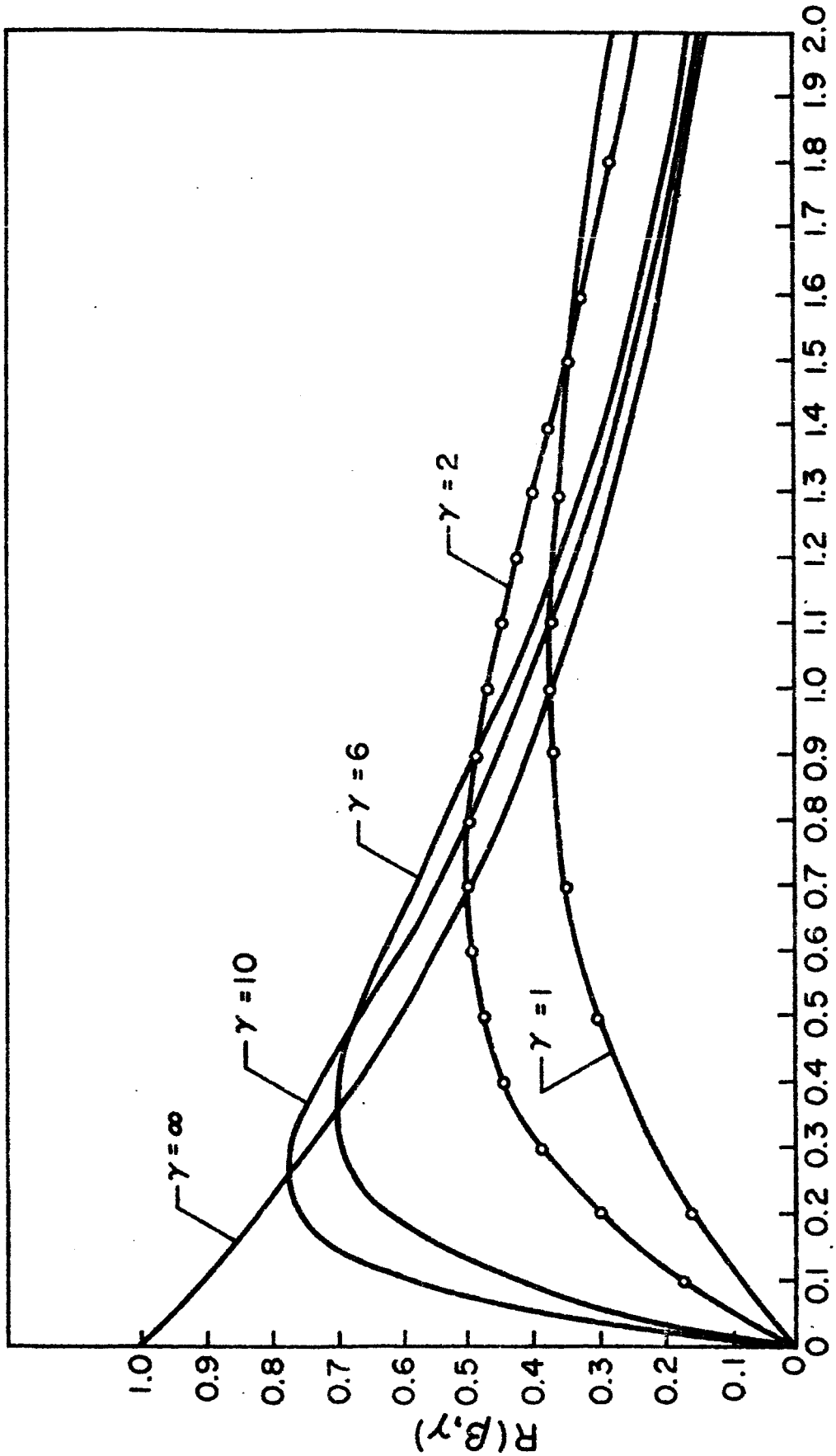
RESPONSE CURVE, LINEAR PLOT
R(β,γ)
β
γ = ∞
γ = 10
γ = 6
γ = 2
γ = 1
0
0.1
0.2
0.3
0.4
0.5
0.6
0.7
0.8
0.9
1.0
1.1
1.2
1.3
1.4
1.5
1.6
1.7
1.8
1.9
2.0

Figure 6a

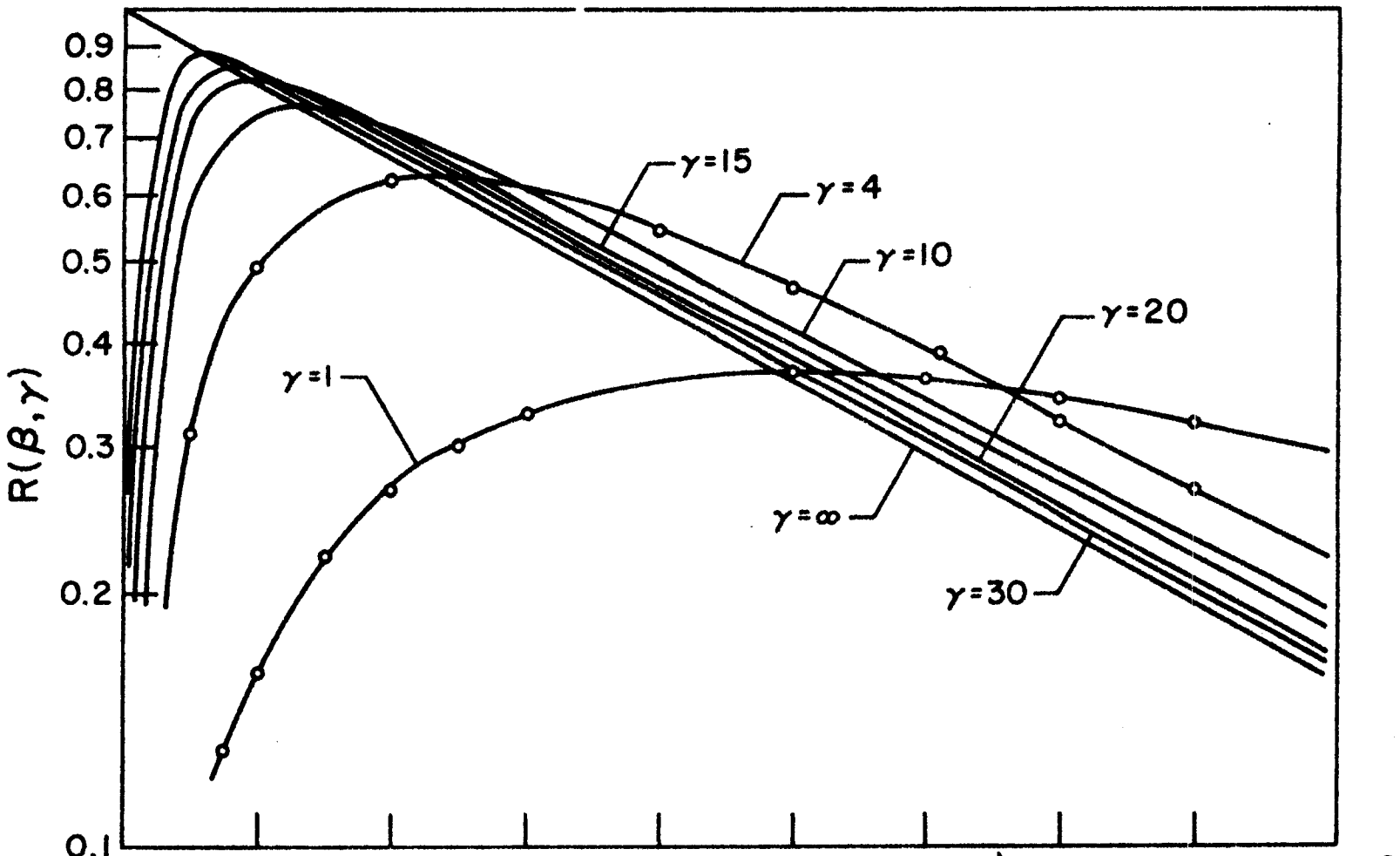

RESPONSE CURVE, SEMILOG PLOT

Figure 6b

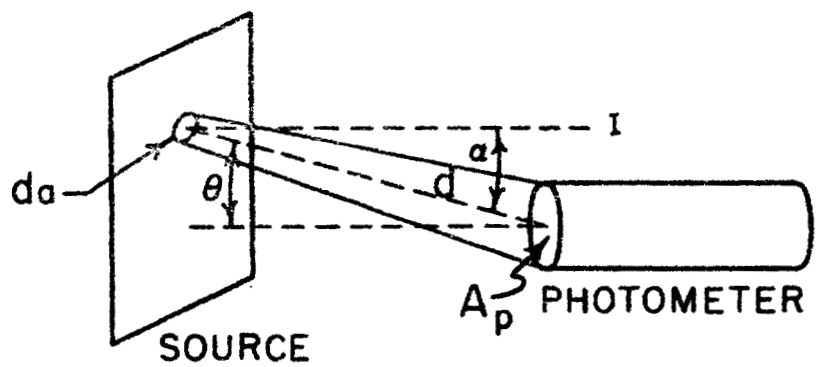

Figure 7.

$$C_{pc} = I_c \, A_p \, \omega_{2eff} \, S_p \, (\lambda_c) \quad . \qquad (4\text{-}22)$$

Finally, we get an expression for ϵ:

$$\epsilon = \frac{4_\pi \; A_T}{\tau \omega' {}_{eff} A_T} \frac{\mu}{\mu c} \cdot \frac{s_p \, (\lambda_c) \int I'(\lambda) \, d\lambda \, C_{Tc}}{\int I' \, (\lambda) \, s_p \, (\lambda) \, d\lambda \, C_{pc}} \cdot \frac{\lambda c}{\lambda} \frac{1}{R} \frac{C_p}{C_T} \quad . \qquad (4\text{-}24)$$

The meanings of different symbols used are given in the report by Bruner.[6] This expression will be further simplified later on in view of the experimental limitations.

CHAPTER II

A BRIEF DESCRIPTION OF THE APPARATUS

The Vacuum Spectrograph

The main instrument employeed in this work was a grazing incidence vacuum monochromator with a fixed grating of one meter radius and having 6000 lines/cm. A traveling stage was driven along the Rowland circle such that the plane of a slit mounted upon it always faced the grating (Figure 8). The spectrometer has been described fully by other investigators.[3,6,12,33]

A pressure of about 5×10^{-5} mm of mercury was achieved by a Kinney KC -15 mechanical pump, a CVC model MC 500 oil diffusion pump (cooled by liquid nitrogen) and another water cooled oil diffusion pump CVC model MC 275. The entrance and the exit slits (windowless) were nearly 500 microns wide; so that the thermopile and the photometer could produce measureable response signals. These large slit sizes, of course, would have resulted in loss of resolution, but for the fact that the spectrum in this experiment consisted of widely separated lines.

The UV reflectivity of the grating was improved by about 33% by depositing evaporated platinum on it. A sputtering technique of this type was used by Watanabe.[2] A pure platinum wire coiled in itself was inserted at the axis of the hollow cathode of the UV source (the Schueler lamp described in the following section) by the investigator, and while the source was operating, its entrance window was opened. In this way, platinum was coated on the grating surface at the place where it is most needed.

The Schueler Source

Newburgh[28] and his associates have described a Schueler source, a hollow cathode discharge lamp, for the production of UV lines from ionized atoms. The main features of the one (a slight modification of Newburgh's design) made by the investigator to suit the present experimental needs are given in Figure 9. The cathode (open at both ends) is constructed from a pure, hollow graphite cylinder about half an inch in outer diameter and having a thick wall. The four stainless steel (about 8 inches long) rods

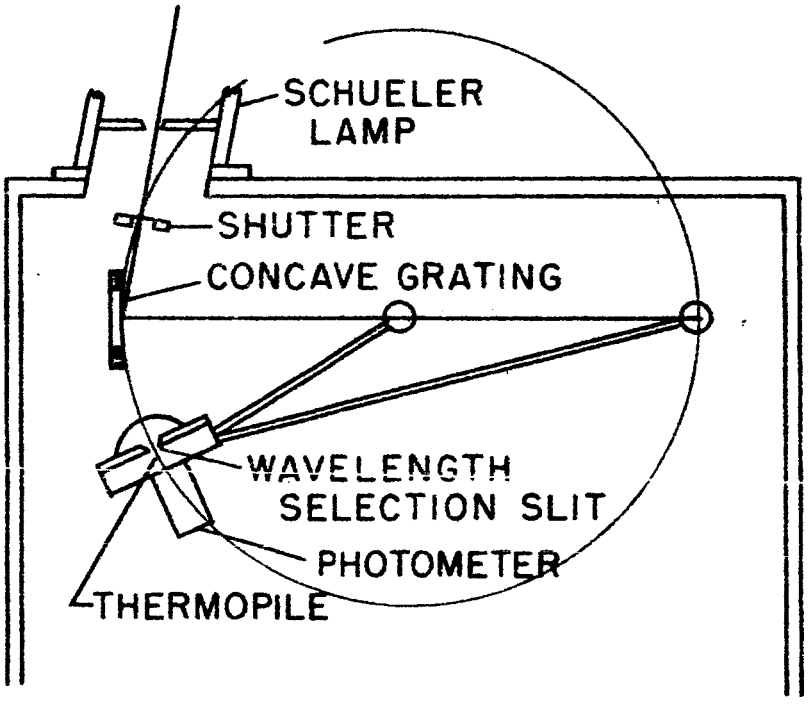

Vacuum Monochromator

Figure 8.

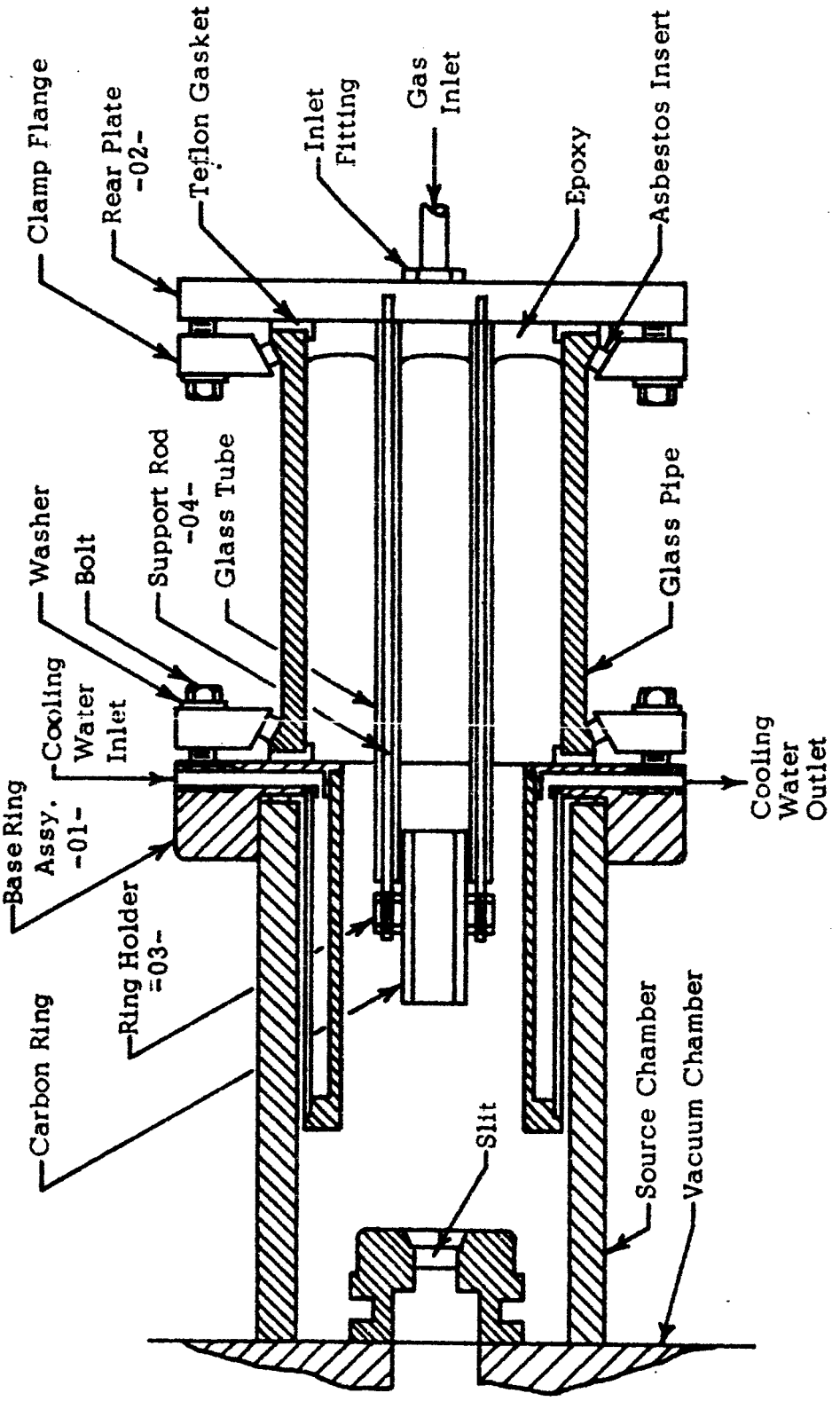

Fig. 9 Schueler Lamp

doubly covered with a quartz tube were provided to conduct power. These were kept in shape and fixed in position by the use of a superior type "epoxy."

Most intense discharge glow between cathode and the surrounding walls of the anode takes place at the axis of the hollow cathode. When the stop cock is opened, the radiation enters the main spectrometer chamber. The pressure in the source tube is maintained at about .17 mm of Hg, for any gas under discharge. This pressure is regulated through a number of needle valves in the source control cabinet and recorded by a Pirani gauge. The gas entering into the monochromater through the stop cock (windowless) is directed towards the mouth of the diffusion pump and is constantly pumped out to maintain sufficient vacuum in the large chamber. The intensity of the line depends upon the source current and pressure. However, to avoid self-absorption, the pressure should not be excessive.

The Source Control Cabinet

As shown in Figure 10 and also mentioned in detail by Bruner,[6] The source control cabinet is a portable rack containing electrical controls for power supply, Pirani gauge, and the source gas metering system made by Bruner[6] (see Figure 11). The pressure of the gas flowing into the Schueler source through two needle valves was regulated well enough that even after long periods of operation there was no noticeable drift in the intensity of the spectrum lines. The line diagram for the gas metering system is given in Figure 10. A mixture of two different gases can also be prepared and fed into the Schueler source for discharge. It was interesting to observe that a mixture of 30% hydrogen and 70% helium quenched the molecular bands of the former and thus the atomic line 1216 A (the hydrogen Lyman alpha line) in the UV was essentially isolated.

With a view to secure a comfortable signal to noise ratio in recorders, it was essential to keep the source stable. Moreover, the observations for the incidnet photons impinging upon, and the luminescent radiation emerging out from the phosphor are made after the lapse of some time interval. The two measurements should be quite consistent. Therefore, a "cartesian manostat," manufactured by the Manostat Corporation, and

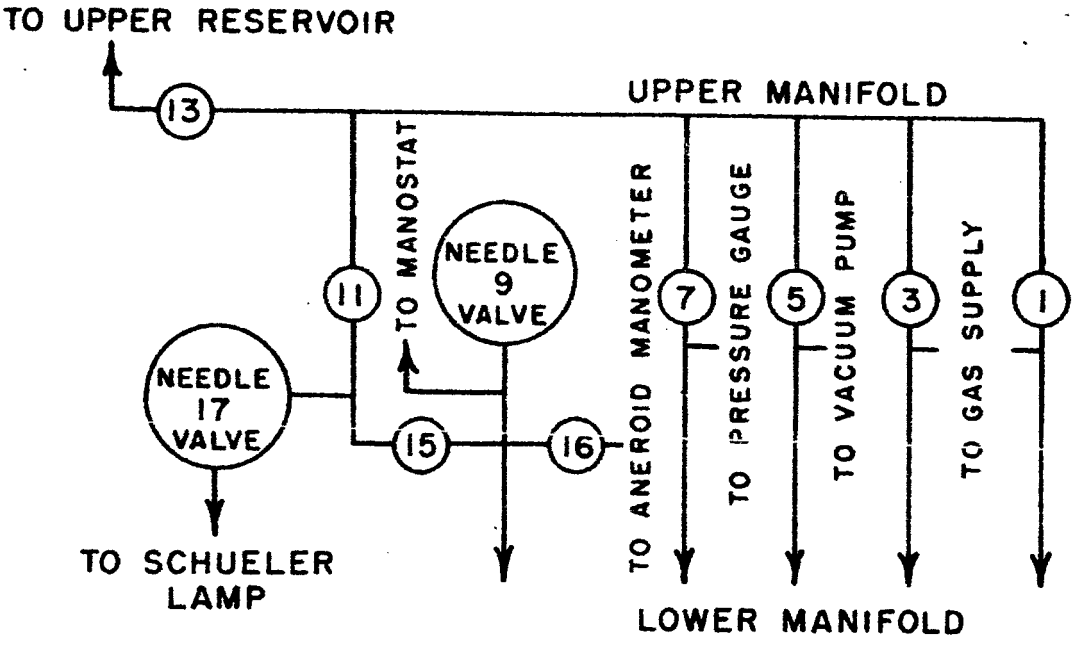

Gas Metering System. Upper Manifold only.

Figure 10.

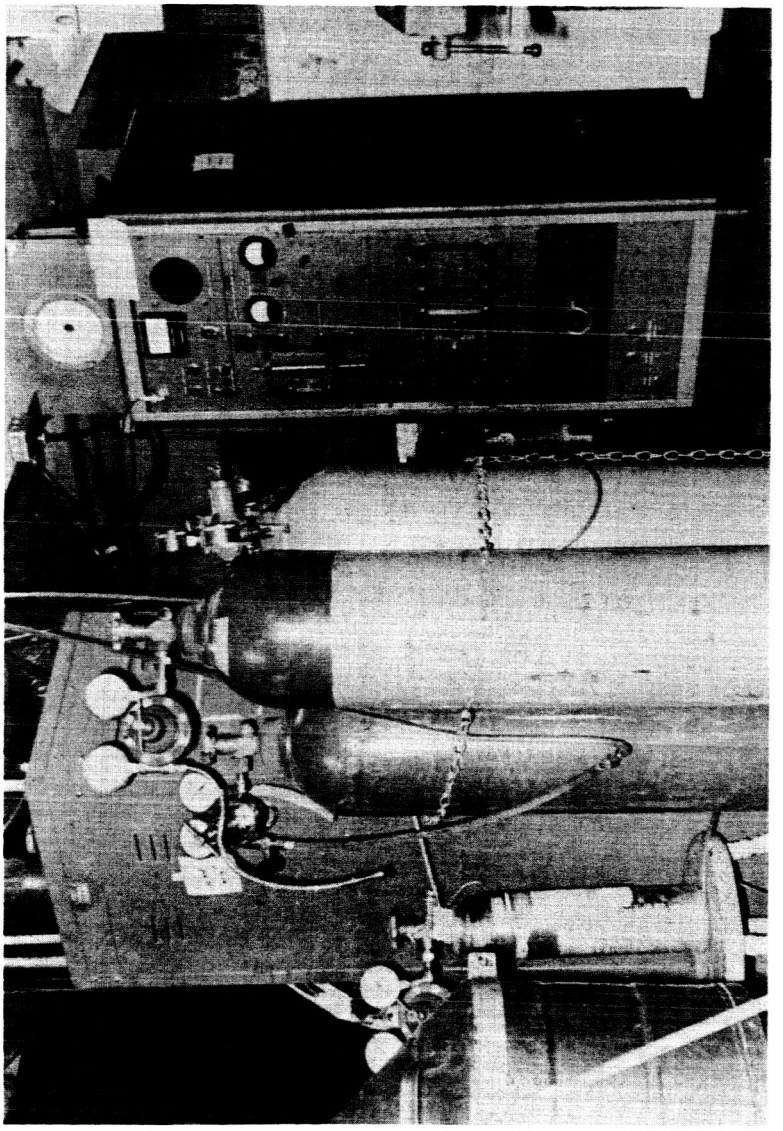

Figure 11.

Gas Metering Manifold and Power Supply Cabinet.

described fully in Bruner's report[6] was used in the gas metering system. By its proper adjustment and careful usage, a fairly constant pressure can be maintained in the ionizing gas inside the Schueler source.

An example will make the operation clear (see Figure 10). Suppose we have to observe the 304 A of helium. We evacuate the whole upper manifold and rinse it with helium and again evacuate it. Then we allow helium gas at 1000 mm of Hg to enter through either valve 1 or 3, closing 5 of course. Needle valve 7 is opened to control the flow of helium through the cartesian manostat at 50 mm of Hg. Finally one allows the gas to flow through valve 17 into the Schueler source. The reading of the Pirani gauge in this case sould be about 0.19 mm of Hg, although upon opening the stop cock, the pressure may drop down to an acceptable value of about 0.17 mm of Hg where it remains when adjustments are properly completed.

The Power Supply

The power supply, mounted on a portable rack, has a transformer (input 220 volt and output 7500 volt), a rectifer unit (two 872 A RCA, mercury vapor rectifying tubes in conjunction with a 0.1 mocrofarad capacitor) and a bank of twenty-five 100 watt, 120 volt filament lamps connected in the series configuration to serve as a ballast resistor. It produces about 4000 volt DC at 1.0 amperes. The simplified circuit is shown in Figure 12 along with the high voltage cable up to the terminal of the Schueler source.

The 600 mA current controlled by means of a variac is best suited for maintaining a stable discharge of all the gases for this work (except argon and neon for which it should be less). The filaments of the two 872 A RCA tubes are heated by a 5 volt AC supply as shown in the diagram. A safety plug was also fitted in the HV circuit to avoid accidental shock while repairing.

Densitometer Photometer and Accessories

The photometer unit was required to find out the values of β for the different samples of phosphor ($Ca\ WO_4$:Pb). It includes a high pressure quartz Hg vapour lamp, a Corning red-purple ultraviolet-filter, a thick phosphor screen and an Aminco Model No. 10-213 densitometer photometer.

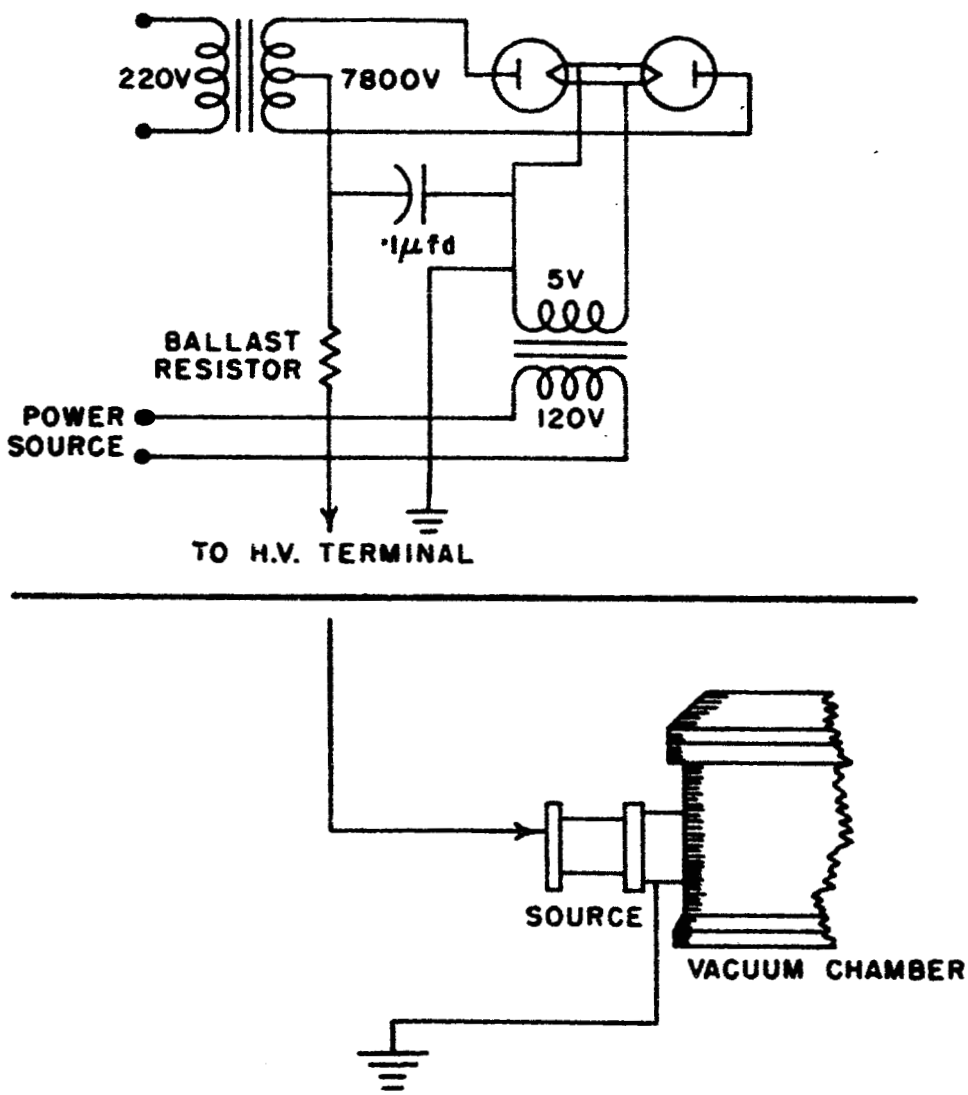

THE POWER SUPPLY

FIG. 12

The Hg lamp and the filter provided UV energy to excite the phosphor in the same way as they would be illuminated in the actual perfomance.

A large number of Ca WO_4:Pb samples of varying thicknesses were prepared, with the use of microscope cover glasses as substrates (22 mm by 22 mm). A solution of the phosphor was prepared in isopropyl alcohol and poured on the substrates and allowed to dry. Areal densities of the depositions were measured by weighing them (Table No. 1). Some of the samples were made by the spraying method.

A rectangular aperture (smaller than the cover glass) was tied securely before one of the thick phosphor screens. The densitometer photometer amplifier was adjusted to read full scale, i.e., zero density, when the source operated without any sample in the optical train. The different samples were then placed behind and photometer readings noted. The densitometer was calibrated directly to read optical density. A graph was plotted from Table No. 1 (see Figure 16). The resulting straight line cut the ordinate at a point whose reading, when subtracted from the total readings, gave the optical density of the phosphor regardless of substrate material.

Thermopile and Accessories

The investigator used a thermopile purchased from Charles M. Reeder and Co., Michigan. Some of its details are given in a paper by Brown,[32] but the advantages and disadvantages are dealt with in a different paper by Samson.[4] The one used here had five junctions, each about 1 mm by 2 mm. These are made of thin gold strips and blackened with evaporated colloidal gold. There are compensating junctions also but these were not used in this experiment. The response from the thermopile is fed into a Liston-Becker amplifier (which is a D.C. breaker amplifier) model 14, Stamford, Connecticut. The output is recorded by an Esterline Angus strip chart recorder, model AW, Indianapolis, Indiana. (See Figure 13). The response of the thermopile (in a vacuum) is measured in microvolts per microwatt.

A motor driven switch which interrupts the input signal from the thermopile eight times per second forms the heart of the DC breaker amplifier mentioned above. As a result of this switch, the square wave so

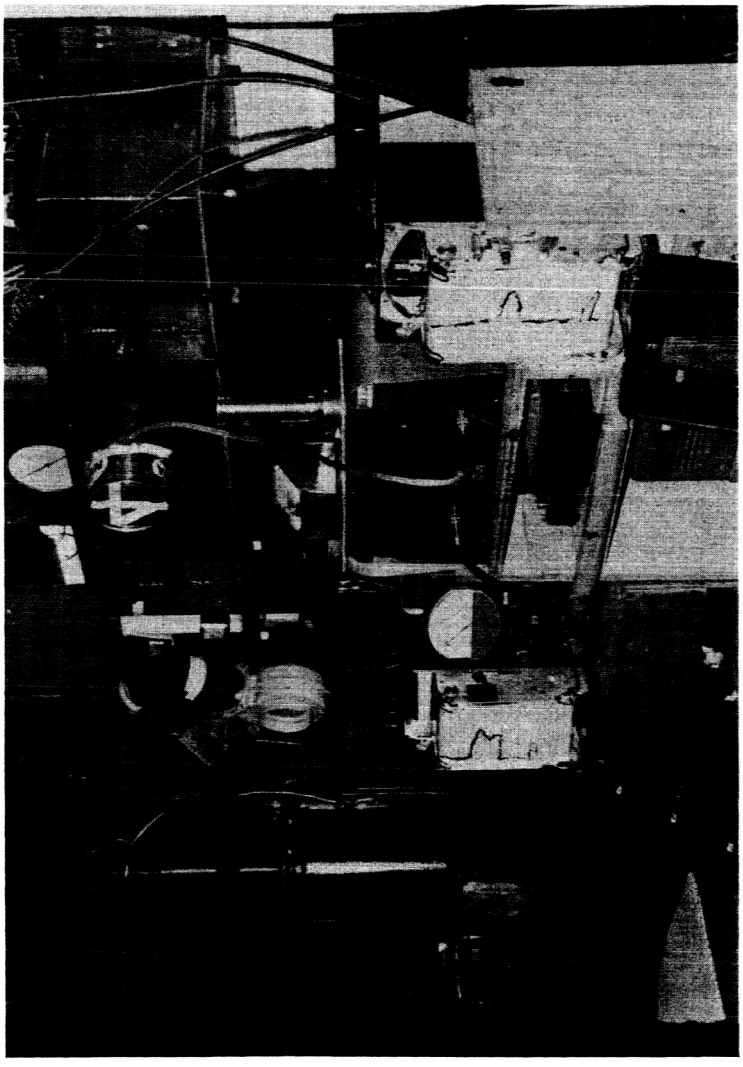

Figure 13.
Thermopile Amplifier and Recorder.

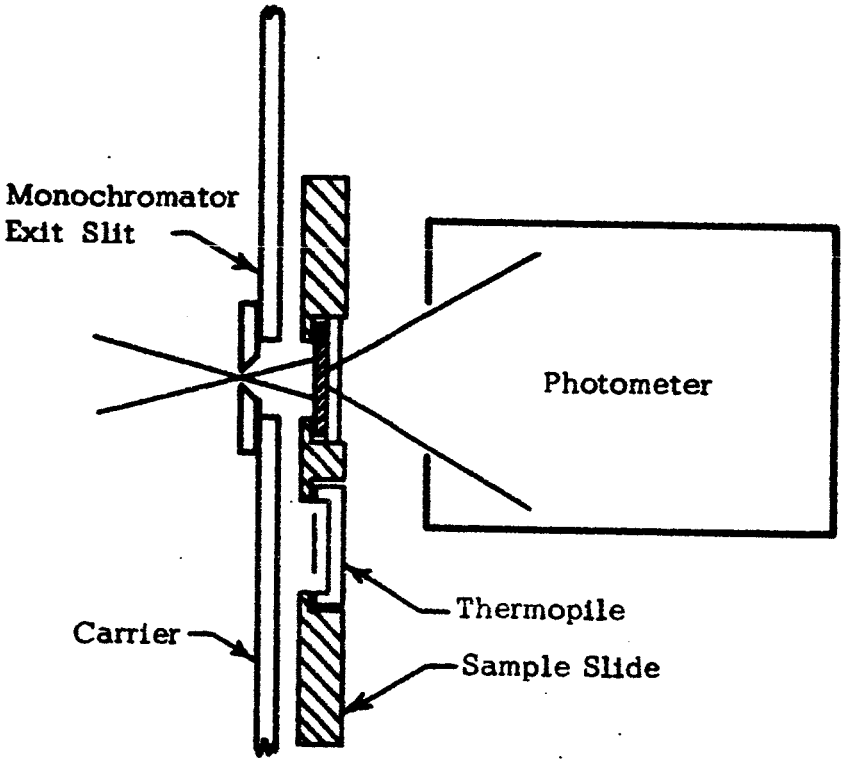

Fig. 14(a) Sample in Position Behind Slit

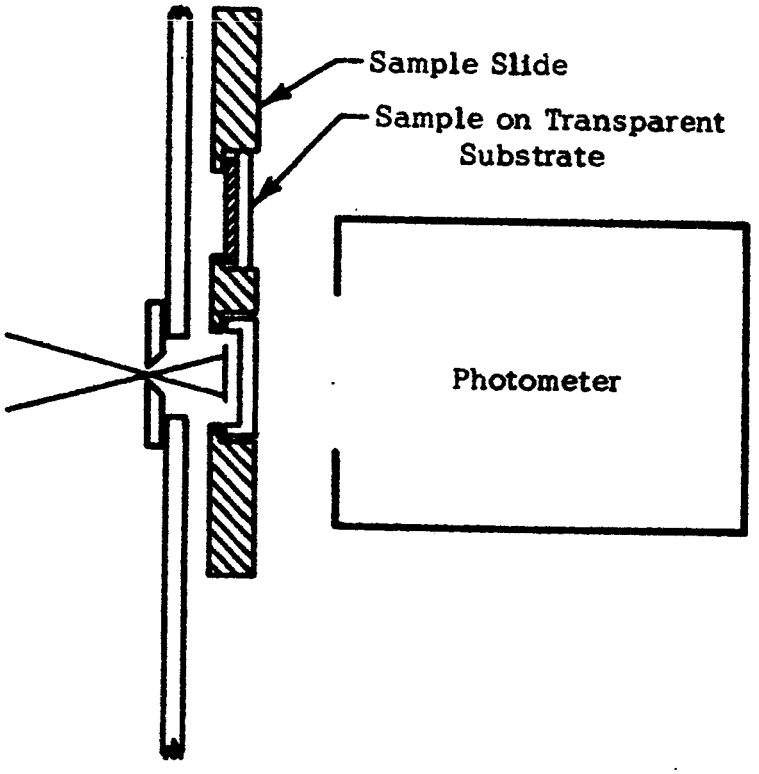

Fig. 14(b) Thermopile in Position Behind Slit

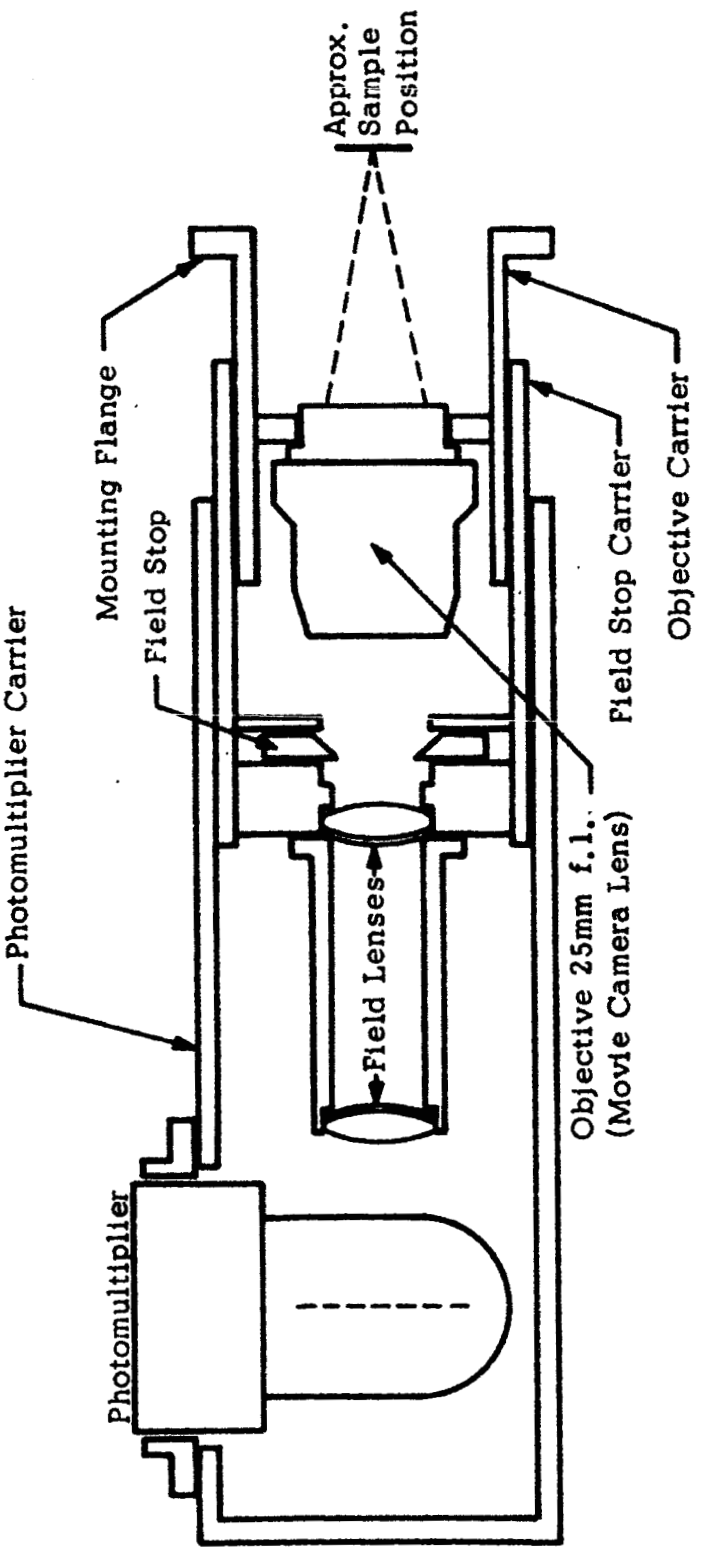

Fig. 15 Photometer Mechanical Arrangement

TABLE NUMBER 1.

Sample No.	Areal Density	Optical Density Phosphors & Substrate.	Optical Density of Phosphors.	β
1	12.91	.97	.39	.9
2	5.33	.73	.15	.3
3	12.04	.94	.36	.82
4	10.78	.97	.39	.9
5	4.21	.63	.05	.11
6	11.61	.94	.36	.83
7	9.30	.97	.39	.9
8	9.05	.85	.27	.62
9	5.41	.73	.15	.3
10	13.07	1.15	.57	1.3
11	6.72	.64	.06	.14
12	11.37	.91	.33	.75
13	23.92	1.32	.74	1.7
14	5.57	.63	.05	.11
15	6.82	.61	.03	.07
16	9.30	.65	.07	.16
17	8.06	.90	.32	.74
18	7.44	.62	.04	.09
19	7.2	.78	.20	.46
20	6.7	.66	.08	.18

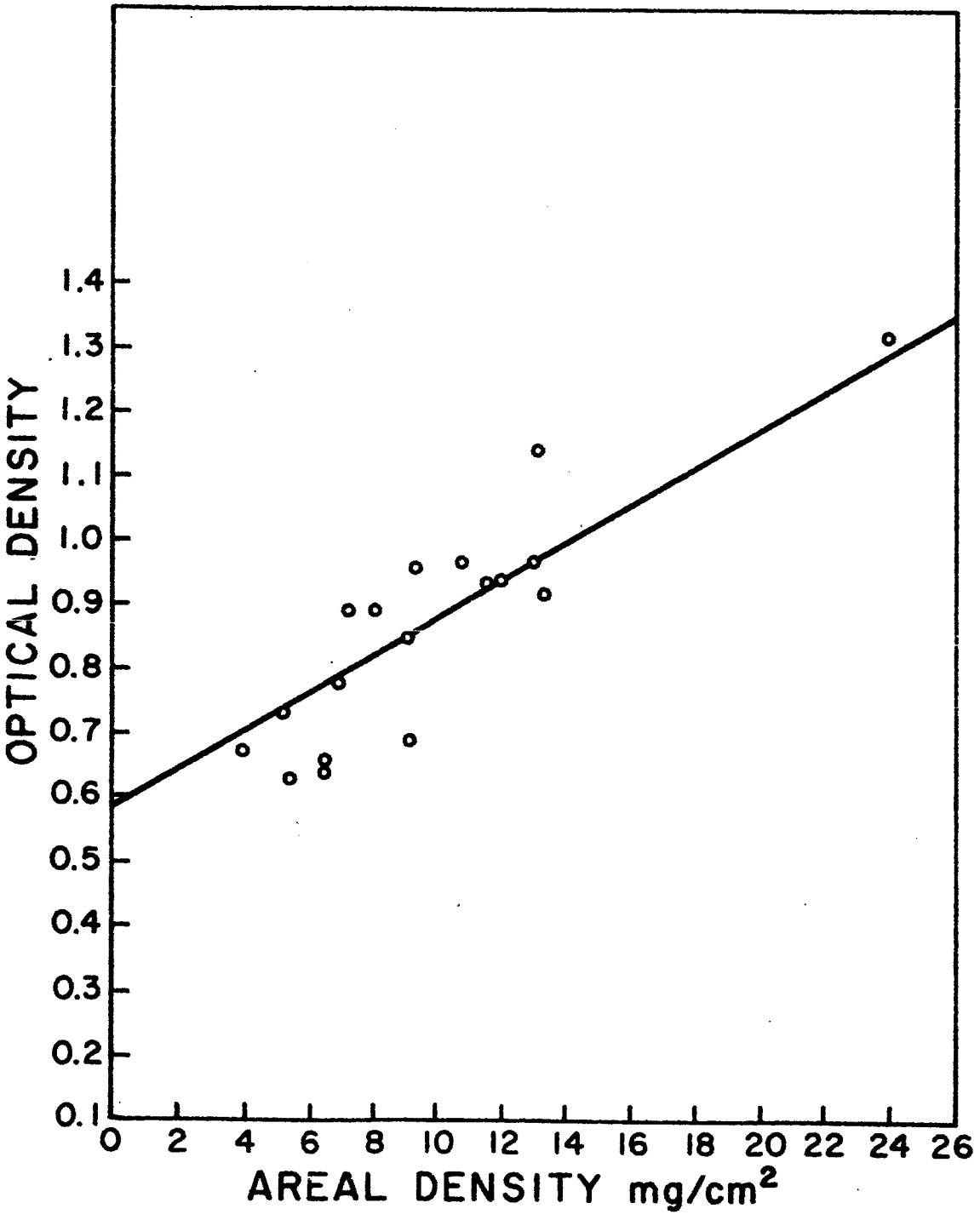
OPTICAL DENSITY
1.4
1.3
1.2
1.1
1.0
0.9
0.8
0.7
0.6
0.5
0.4
0.3
0.2
0.1
0
2
4
6
8
10
12
14
16
18
20
22
24
26
AREAL DENSITY mg/cm²

Figure 16

generated is fed into a powerful amplifier and then into a synchronous switch for final rectification. In this way the thermopile response signal is sufficiently amplified and reproduced on a constantly moving chart by a fine recording pen. In order to shield the noise currents of the order of a few mocrovolts, a metal can was used. The worker has to wait for quite some hours till the chamber does not show any significant pressure and temperature variations which cause the noise.

The probability of energy loss due to the photoelectric effect termed here as "photoelectric-cooling" was not ruled out completely in view of the fact that the work function of the thermopile material is less than the energy of the UV photons used to excite luminescence. Bruner[6] devised a unique technique of "retarding potentials" to verify the otherwise unaccounted for loss of energy and to make subsequent corrections. But fortunately so little "cooling" was detected that the effect could be ignored in the final computations.

The Sample Holder

As shown in Figure 14a and 14b, the sample holder is a plate made of brass which contains two openings: one for the thermopile and the other for the photometer. The opening pieces can be positioned behind the exit slit one after the other by sliding them into a groove of another big brass plate mounted on the scanning arm table. This was achieved very accurately by means of a remote control threaded axle of a 28 DC motor and two limiting microswitches. The center of the exit slit was constrained to move along the Rowland circle.

The Photometer

The photometer was specially designed by Bruner[6] (see Figure 15) to suit the requirements of this particular experiment in the work shop of the department. A 1.9 camera lens was used as an objective, along with two suitable lenses and a rectangular field stop. The luminescent radiation from the phosphor was finally focussed on the cathode of the 931 A RCA photomultiplier tube by means of several appropriate adjustments. At the end of the outer cylinder behind the phototube, a red test lamp was fixed. It could be lighted up and its intensity controlled by a switch outside the

chamber for frequent measurement verifications. The other details are given in Bruner's report.[6]

The high voltage power supply for the photometer was such that it produced about 800 volts to be delivered to the base of the 931 A tube. The General Radio 1230- A DC amplifier and electrometer was used to measure the current which is related to the luminescent intensity. This current was recorded on an Esterline - Angus chart, similar to that used in the case of the thermopile. The sensitivity of the electrometer can be changed by means of an input resistance. The dark current, or the so called background intensity of the tube selected for this work, was very small and, as such, it provided dependable data.

The Experimental Procedure

After removing the grating cover, one of the phosphor samples and the photometer were positioned behind the exit slit. The vacuum chamber was then evacuated by using all the pumps in the required order until the Philips Pressure guage PHG-09 (Consolidated Vacuum Corporation) recorded about 5×10^{-5} mm of mercury. The Schueler source and the upper part of the gas metering manifold were rinsed with the gas to be used and then evacuated. The gas was then allowed to enter the Schueler source and the latter fired. The ionization current in the plasma was kept at 600 mA. Usually, it requires about 30 minutes time to stabilize the source. The power for the thermopile and photometer recorders was already turned on four hours in advance.

The exit slit at the scanning arm was set very near to the monochromatic radiation in question. When all worked satisfactorily for some time, the entrance slit was opened. At this stage the pressure of the chamber changes a little; because the Schueler source requires a higher pressure than the chamber. However, the newtral gas is directed toward the mouth of the big diffusion pump and so carried away without disturbing the vacuum of the chamber to a large extent. The sensitivity of the amplifier electrometer is adjusted and the monochromatic raidation is scanned completely. Several readings of such scans were taken. The checks were made by the test lamp.

Afterwards, the phosphor sample is shifted aside and the thermopile takes its place. When the thermopile establishes a radiative steady state with the walls of the chamber and other surroundings, the intensity of the irradiance is measured. The investigator has to invariably use about four black shields on both the sides of the monochromatic radiation path between the grating and the exit slit in front of the thermopile. In this way, stray light reflected from the walls of the chamber can be cut off. A constant value internal signal was put on frequently to check the responsitivity of the Liston-Becker amplifier.

Observations as described above were made for all the samples at five different UV spectral lines known to be fairly intense, i.e., 304 A of helium, 461 A of neon, 584 A of helium, 1048 A of argon, and 1216 A of hydrogen.

The Intercalibration

The light from the quartz mercury discharge tube operated by a Sola Constant Voltage transformer was allowed to fall on an opal glass piece, 3/4 square inch, and the diffused radiation then allowed to pass through a Wratten 77 A filter which isolated the 5461 A. A bottle of copper sulphate solution was kept in the optical train to remove the infrared radiation which otherwise would effect the thermopile response. With the use of these filters and a metal shutter, the background intensity was also noted. The thermopile was four inches away from the opal glass. Observations were made with the exit slit removed and the chamber evacuated.

Afterwards, the thermopile was removed and in its place the photometer was so oriented that its object plane coincided with the diffuse surface of the opal glass. Of course, a neutral density filter was sandwiched between the two to reduce the signal strength. Several readings were taken with this arrangement without evacuating the chamber.

It was felt during the course of experiment that the copper sulphate solution was not completely cutting off the infrared and, therefore, a Wratten 25 filter in addition to the other elements was introduced. This filter is supposed to quench the 5461 A of mercury completely but to pass the the infrared. This revealed that about 13% of the infrared does

penetrate through the copper sulphate solution, and so it was accounted for in the thermopile readings for the purpose of final calculations of the quantum efficiency.

In order to find the ratio of ω_{2eff} and ω_{1eff} (see Eq. 4-24) a photograph was obtained while the photometer remained positioned behind the slit plus the phosphor sample, and the direct reflected light from the grating provided the illumination for the camera. The areas were measured by the Keuffel planimeter (see Figure 18) upon an enlargement of such a photograph.

CHAPTER III

ANALYSIS OF THE DATA

The value of β (thickness parameter) for each sample was found from the experimental curve (optical density vs. areal density) with the help of the relation: $\beta = D/\text{Log } e$, where D is the optical density of the phosphor only and can be obtained by subtracting the density of the substrate which, in our case, is taken to be the point where the experimental straight line intersected the Y-axis (see Figure 16).

Next step was to draw the semi-log type graph (relative response vs. β - the thickness parameter) for each sample on the same five UV wavelengths and then match them with the theoretical curves drawn earlier on the same scale. In order to do this, the values of relative response, r, (not the R which is response function; because the value of γ is yet to be fixed by matching the experimental and theoretical curves on the same scale. That is why 'r' has been tentatively used in place of 'R') defined below were calculated from the observed data.

$$r \equiv \frac{\overline{P}\ \overline{TT}}{\overline{T}\ \overline{PT}}$$, where $\overline{P}$ is the average of the photometer readings, $\overline{PT}$ is the average of the test lamp readings, $\overline{T}$ is the average of the thermopile readings and $\overline{TT}$ is the average of the thermopile amplifier test signal readings. In this case all checks were done by a 0.1 micro-volt internal test signal.

Upon drawing the curves, it was found that they could be easily matched with the theoretical curves between R and β.

It may be mentioned here that the photometer amplifier sensitivity was kept at 3×10^{-9} amps throughout the course of measurements, while for the PT measurements the lamp current was 54 mA. However, for intercalibration the sensitivity was fixed at 3×10^{-8} amps, 1.e., 0.1 of the previous value.

Similarly the coarse gain setting of the Liston-Becker amplifier for use in recording the thermopile response was constantly kept at 18, fine gain at full scale, and the position range at 3. A 0.1 micro-volt internal signal was used to evaluate the value of $\overline{TT}$.

The approporiate gases were introduced into the Schueler source at a constant pressure of 0.17 mm of Hg and the ionization current was maintained at a fixed value of 600 mA in all cases except for argon.

The final measurements consisted in determining the rest of the parameters in the expression for ϵ. The integrals were evaluated graphically with the help of a planimeter, and with the use of the emission spectrum of Ca WO_4:Pb, from Dr. Conklin's thesis,[12] and the relative responses of the RCA 931 A tube (supplied by the manufacturer) in different wavelength regions (see figure 17 and table 2).

The ratio $\frac{\omega_{2eff}}{\omega_{1eff}}$ was evaluated by taking a picture (Figure 18) of the field stop aperture with the sample illuminated before it by the direct reflected light from the grating and measuring the ratio of the areas with a 4236 M Keuffel and Esser Company (Germany), planimeter. The value of $\frac{1}{\tau}$ was determined from the graph between optical and areal densities (see Figure 16). $A_{T'}/A_T$ was found with the aid of the traveling microscope, and ω'_{eff} was calculated from the dimensions of opal galss and its distance from the thermopile receiver. μ/μ_c was taken to be one for all practical purposes. These values are given in Table No. 3.

The final value of ϵ can be written in the form as below:

$$\epsilon = \frac{F}{10} \frac{\lambda c}{\lambda} \frac{r}{R} \qquad (4\text{-}25)$$

$$\text{where } F = \frac{4\pi}{\tau\, \omega'_{eff}} \frac{A_{T'}}{A_T} \frac{\mu}{\mu_c} \frac{\omega_{2eff}}{\omega_{1eff}} \left(\frac{s_p(\lambda_c) \int I'(\lambda)\, d\lambda}{\int I'(\lambda)\, s_p(\lambda)\, d\lambda} \right) \frac{1}{r_c} r_f \quad ,$$

and where r_c is the relative response found from intercalibration. In fact, C_{Tc}/C_{Pc} has been rightly replaced by $1/r_c$, and r in (4-25) has replaced C_p/C_T. The factor, r_f, is the transmission of the neutral density filter, used for the photometer during intercalibration. The factor 10 takes care of the different settings of the sensitivities of the photometer during the primary data and intercalibration. The thermopile settings were not changed.

The value of $\frac{s_p(\lambda_c) \int I'(\lambda) d\lambda}{\int I'(\lambda)\, s_p(\lambda)\, d\lambda}$ was found from the graph (see Table 2 and Figure 17). The values of γ were found by matching the theoretical and

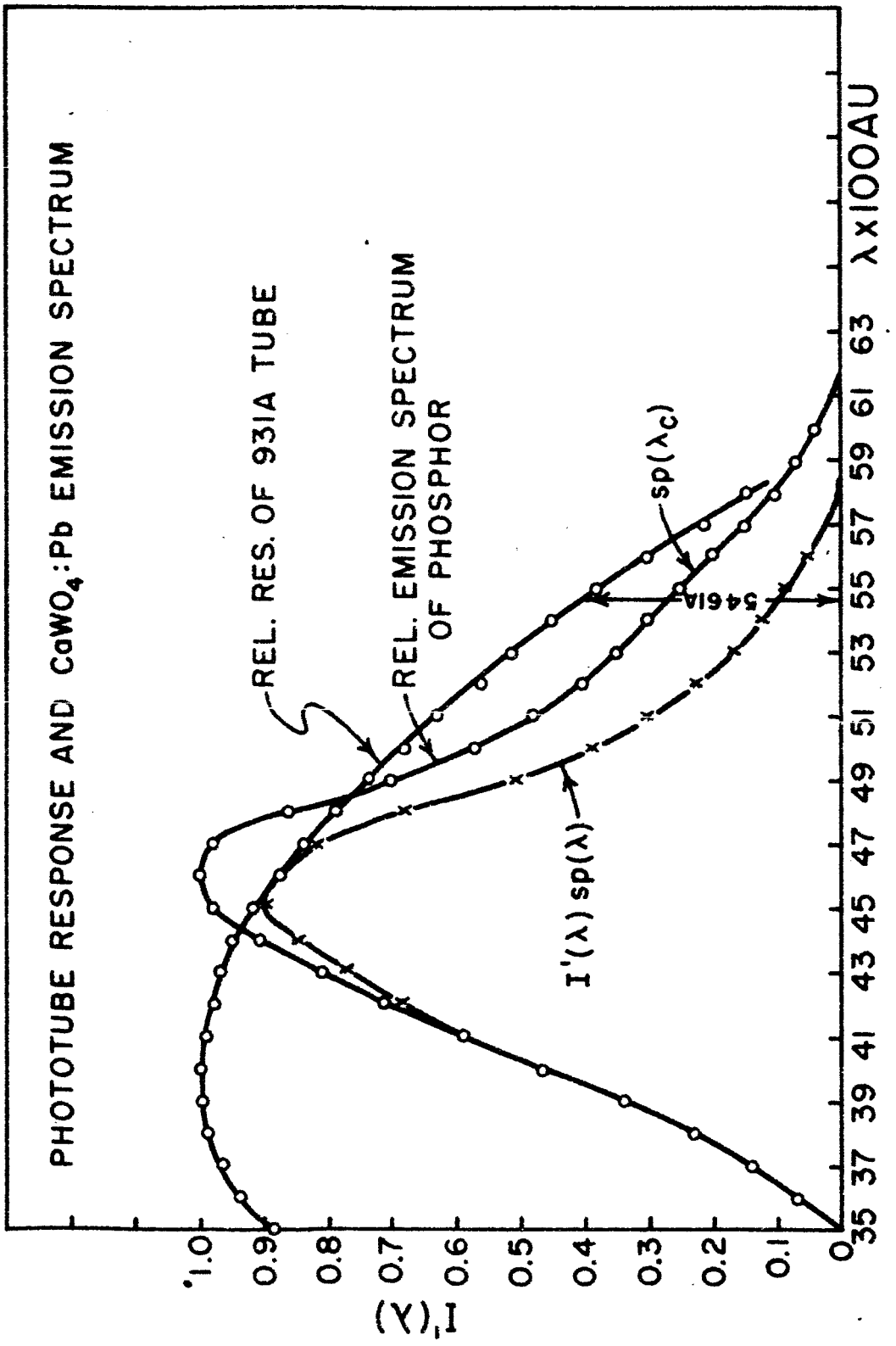
PHOTOTUBE RESPONSE AND $CaWO_4$:Pb EMISSION SPECTRUM
REL. RES. OF 931A TUBE
REL. EMISSION SPECTRUM OF PHOSPHOR
$sp(\lambda_c)$
5461A
$I'(\lambda)\, sp(\lambda)$
$I'(\lambda)$
1.0
0.9
0.8
0.7
0.6
0.5
0.4
0.3
0.2
0.1
0
35 37 39 41 43 45 47 49 51 53 55 57 59 61 63
λ x100AU

Figure 17

TABLE NUMBER 2.

Wavelength Å U.	I' (λ) Conklin's Data.	s_p (λ) RCA-931A	I'(λ) s_p (λ)
3500	.00	.89	.00
3600	.07	.94	.06
3700	.14	.97	.13
3800	.23	.99	.22
3900	.34	1.00	.34
4000	.47	1.00	.47
4100	.59	.99	.59
4200	.71	.98	.69
4300	.81	.97	.78
4400	.91	.95	.86
4500	.98	.92	.90
4600	1.00	.88	.88
4700	.98	.84	.82
4800	.86	.79	.68
4900	.70	.74	.51
5000	.57	.68	.39
5100	.48	.63	.30
5200	.41	.57	.23
5300	.35	.51	.18
5400	.30	.45	.13
5600	.20	.30	.06
5800	.11	.15	.01
6000	.04	.03	.00

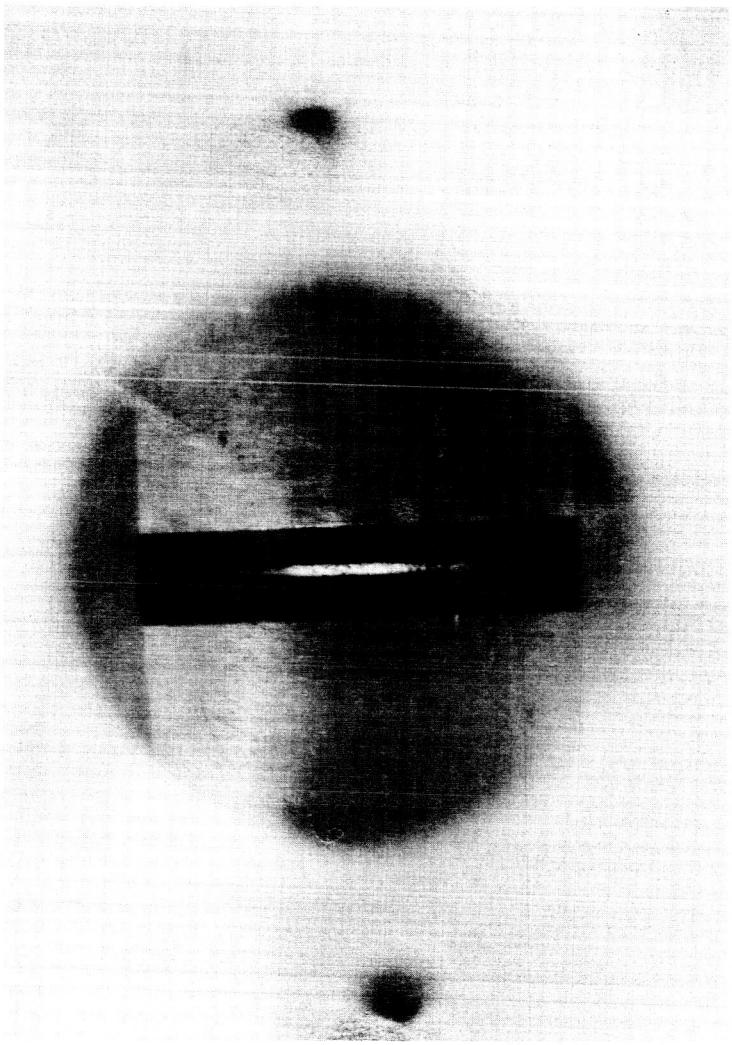

Figure 18.
$\omega_{2eff}/\omega_{1eff}$ Illustration.

TABLE NUMBER 3.

VALUES OF CONSTANTS.

$\frac{A_{T'}}{A_T} = .58$

$\frac{\omega_{2eff}}{\omega_{1eff}} = 8.7$

$r_c = 2.13$

$r_f = .924 \times 10^{-3}$

Optical density of the substrate = .58.

$\omega'_{eff} = \frac{.75 \times .75}{4 \times 4}$

$= .0351$

$\frac{1}{\tau} = 3.802$

$\frac{\mu}{\mu_c} \simeq 1$

$\frac{s_p(\lambda_c) \int I'_\lambda(\lambda)\, d\lambda}{\int I'(\lambda)\, s_p(\lambda)\, d\lambda} = .51$

experimental curves, and in this way the value of R was fixed. Eventually, the value of ϵ was determined at 5 UV wavelengths (see the constants in Table 3).

TYPICAL CHART FOR OBSERVATION OF r

Sample Number 9, β = .3

Obs. No.	Time	Source	Reading	Remarks
1	09.40	P_3	16	P_3-photometer response at 304 A.
2	09.46	P_5	37	P_5-photometer response at 584 A.
3	09.53	PT	18	PT-photometer response at test lamp.
4	10.21	T_3	15	T_3-thermopile response at 304 A.
5	10.45	T_5	28	T_5-thermopile response at 584 A.
6	10.55	TT	25	TT-thermopile response at test signal.
7	11.25	P_3	17	$\bar{P}_3 = 16.75$
8	11.35	P_5	39	$\bar{P}_5 = 39.0$
9	11.43	PT	20	$\overline{PT} = 19.50$
10	12.48	T_3	14	$\bar{T}_3 = 14.75$
11	13.15	T_5	26	$\bar{T}_5 = 26.75$
12	13.30	TT	24	$\overline{TT} = 24.50$
13	14.05	P_3	17	$r_3 = 1.427$
14	14.18	P_5	40	$r_5 = 1.832$
15	14.35	PT	20	
16	15.30	T_3	16	
17	15.48	T_5	25	
18	16.00	TT	24	
19	16.10	P_3	17	
20	16.15	P_5	40	
21	16.25	PT	20	
22	17.20	T_3	14	
23	17.45	T_5	28	
24	18.00	TT	25	

TABLE NUMBER 4.

Summary of data and results.

$F = 1.51$, $\lambda_c = 5461$ Å, $\lambda = 304$ A, *$\gamma = \infty$

Sample	β	R	r	ϵ
1	.90	.4066	.81	5.4036
2	.34	.7082	1.26	4.8270
3	.83	.4364	.808	5.0230
4	.90	--	--	--
5	.11	.8920	1.38	4.1972
6	.83	.4364	.874	5.4330
7	.90	.4066	.891	5.9450
8	.62	.5373	.958	4.8372
9	.34	.7082	1.42	5.4627
11	.14	.8710	1.60	4.9837
12	.76	.4681	1.063	6.1609
13	1.7	.1827	.345	5.1230
14	.11	.8920	1.364	4.1490
15	.07	.9319	1.35	3.9302
17	.74	.4791	.942	5.3342
18	.09	.9120	1.58	4.7010
19	.46	.6313	1.097	4.7140
20	.18	.8340	1.235	4.0174

Av. of ϵ at 304 A = 4.9552.

*(see Figure 19.)

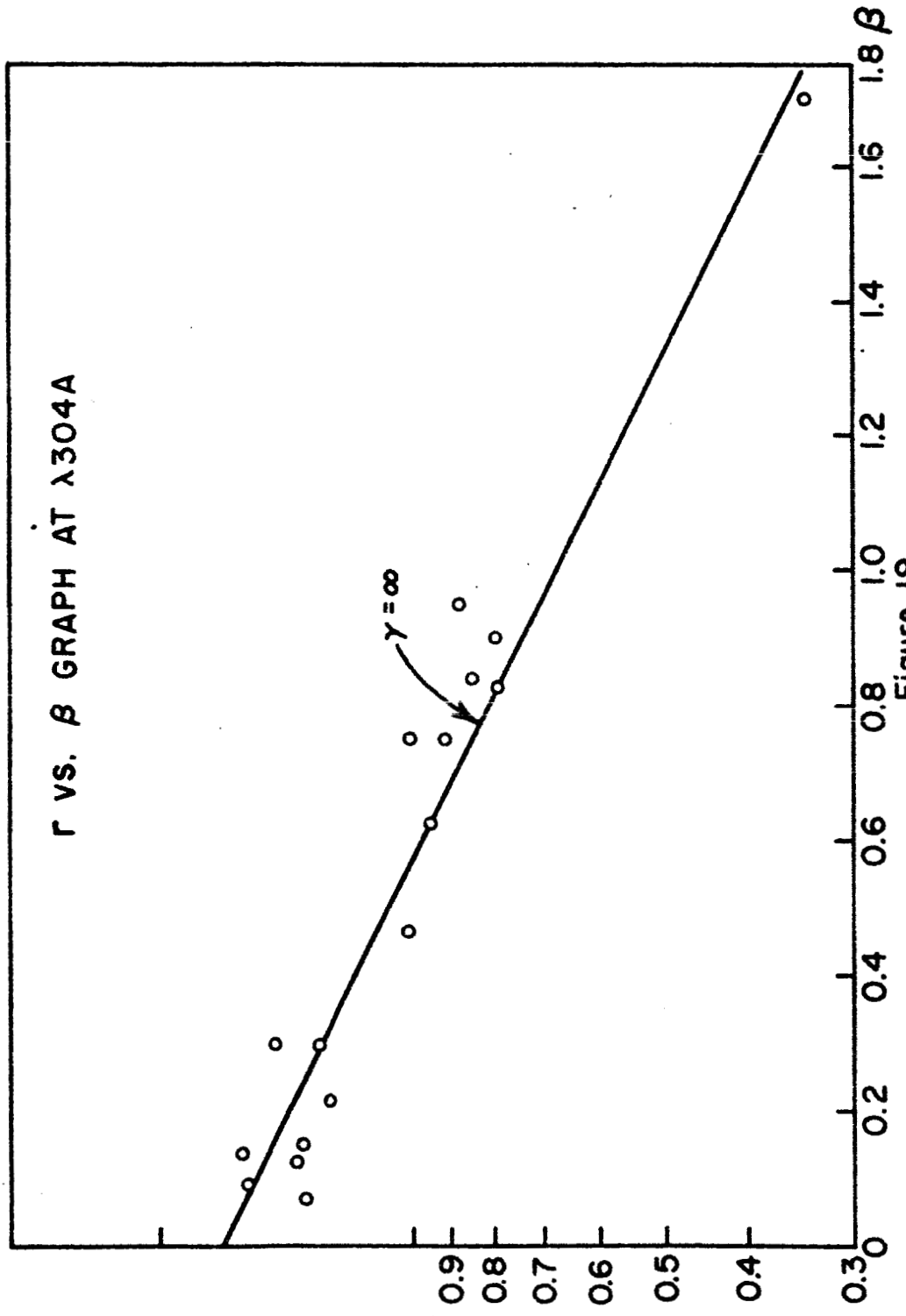
r VS. β GRAPH AT λ3044
γ = ∞
r
0.9
0.8
0.7
0.6
0.5
0.4
0.3
0
0.2
0.4
0.6
0.8
1.0
1.2
1.4
1.6
1.8 β

Figure 19

TABLE NUMBER 5.

Summary of data and results.

$F = 1.51$, $\lambda_c = 5461$ Å, $\lambda = 461$ A, $*\gamma = 30$

Sample	β	R	r	ε
1	.90	.4280	.790	3.3016
2	.34	.7662	1.246	2.9088
3	.83	.4583	.976	3.8094
4	.90	--	--	--
5	.11	.8887	1.800	3.6231
6	.83	.4507	.960	3.8102
7	.90	.4280	1.008	4.2130
8	.62	.8727	1.251	2.5633
9	.34	.7662	1.526	3.5626
11	.14	.8596	1.747	3.6350
12	.76	.4887	1.118	4.0922
13	1.7	.1890	.32	3.0286
14	.11	.8887	1.643	3.3071
15	.07	.8096	1.280	2.8281
17	.74	.4937	1.290	4.6740
18	.09	.8468	1.650	3.4855
19	.46	.6531	1.449	3.9688
20	.18	.8588	1.574	3.2077

*(see Figure 20.)

Av. of ε at 461 A = 3.531

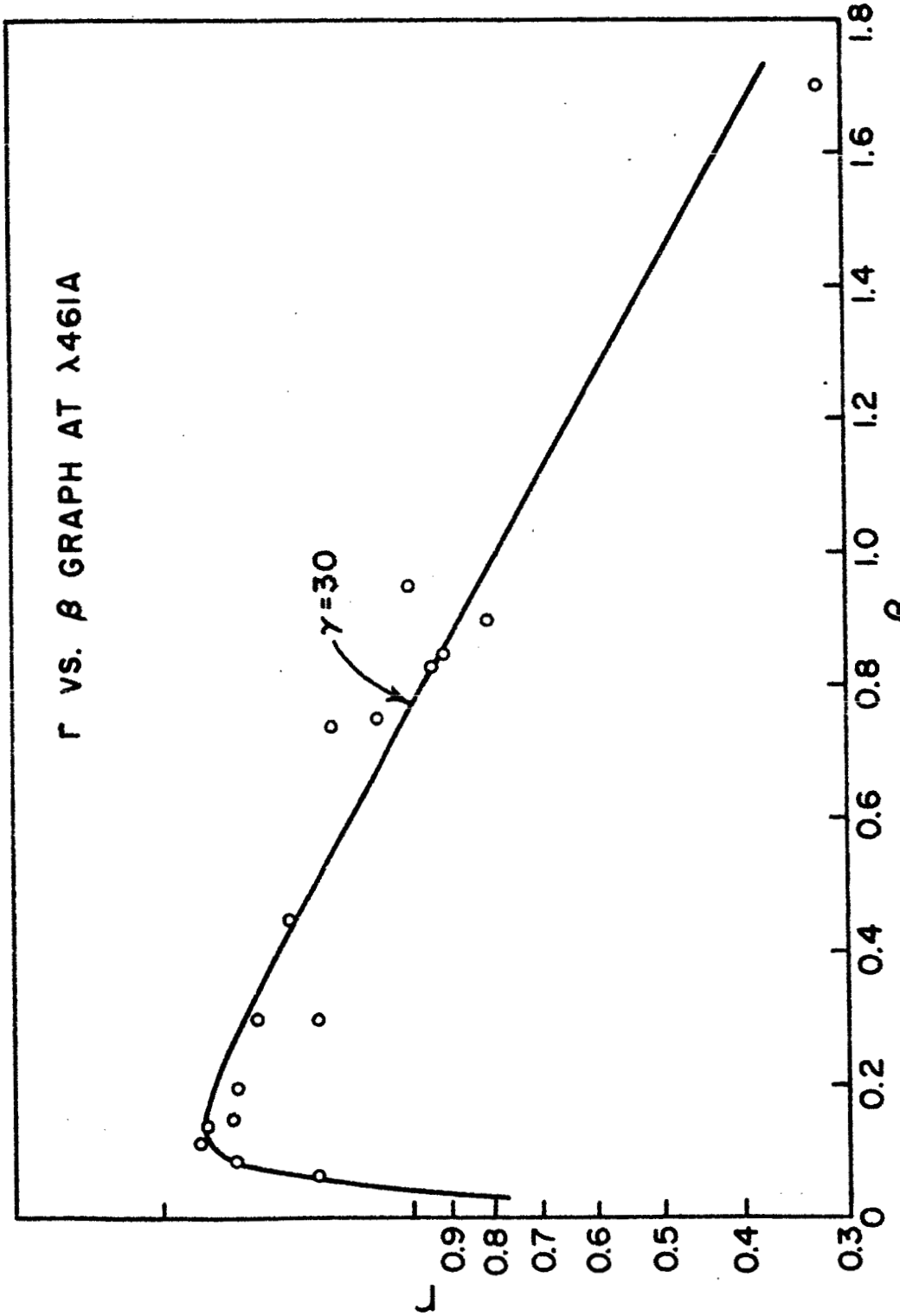
Γ VS. β GRAPH AT λ461A
γ=30
Γ
β
0.3
0.4
0.5
0.6
0.7
0.8
0.9
0
0.2
0.4
0.6
0.8
1.0
1.2
1.4
1.6
1.8

Figure 20

TABLE NUMBER 6.

Summary of data and results.

$F = 1.51$, $\lambda_c = 5461$ Å, $\lambda = 584$ Å, $*\gamma = 20$

Sample	β	R	r	ε
1	.90	.4279	.8591	2.8349
2	.34	.7442	1.653	3.1306
3	.83	.4635	.9685	2.9504
4	.90	--	--	--
5	.11	.8265	1.858	3.1742
6	.83	.8334	1.157	1.9603
7	.90	.4635	.8522	3.3390
8	.62	.5662	1.24	3.0923
9	.34	.7442	1.831	3.5740
11	.14	.8503	1.75	2.9060
12	.76	.4978	1.128	3.1995
13	1.7	.1923	.364	2.6727
14	.11	.8265	2.02	3.4510
15	.07	.7214	1.339	2.6260
17	.74	.5022	1.424	4.0270
18	.09	.7924	1.66	2.9580
19	.46	.6645	1.561	3.3170
20	.18	.8499	1.696	2.8180

*(see Figure 21.)

Av. of ε at 584 A = 3.017

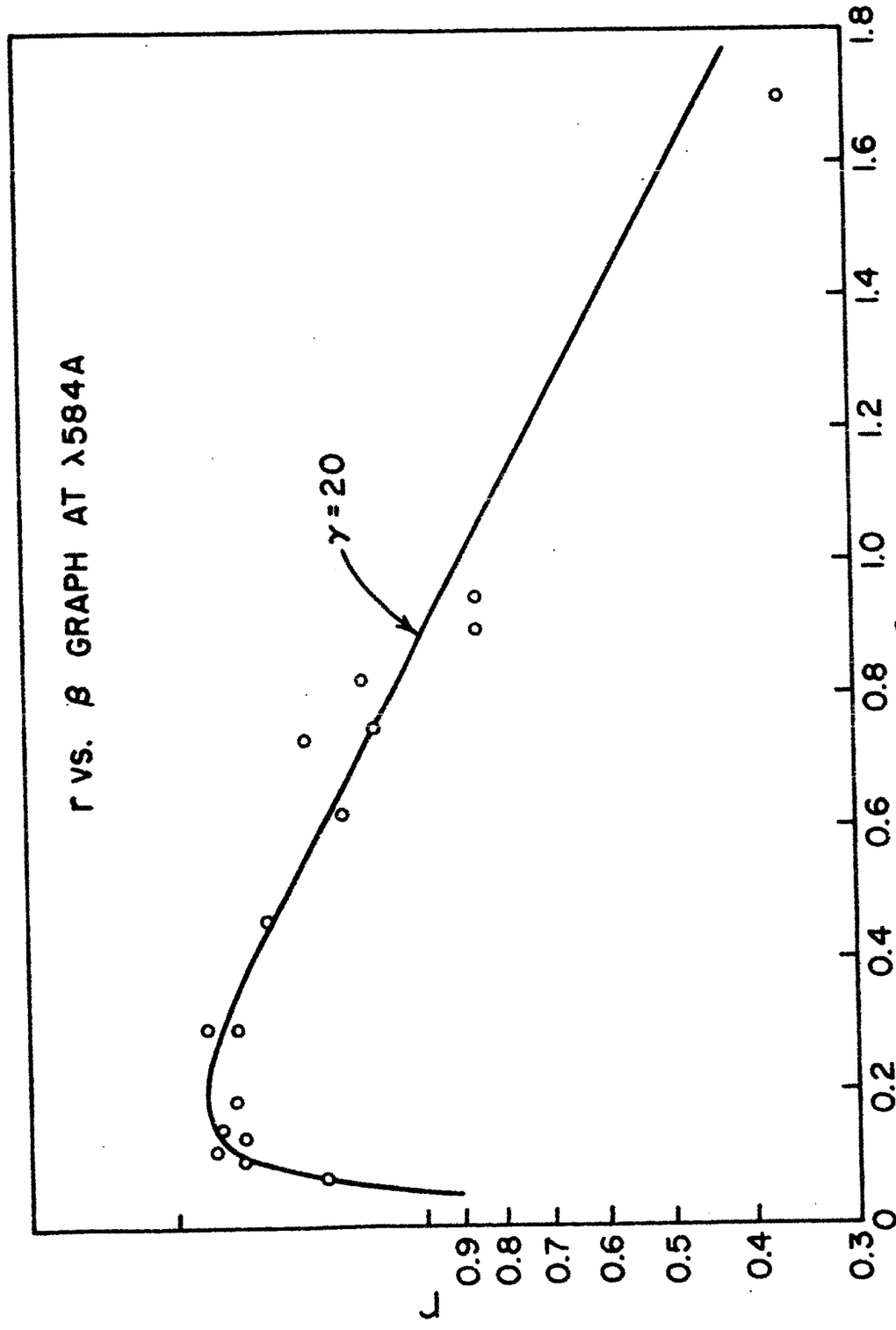
r VS. β GRAPH AT λ584A
γ=20
r
β
0.9
0.8
0.7
0.6
0.5
0.4
0.3
0
0.2
0.4
0.6
0.8
1.0
1.2
1.4
1.6
1.8

Figure 21

TABLE NUMBER 7.

Summary of data and results.

$F = 1.51$, $\lambda_c = 5461$ Å, $\lambda = 1048$ Å, *$\gamma = 15$

Sample	β	R	r	ϵ
1	.90	.4355	.670	1.2105
2	.34	.7819	.910	.9157
3	.83	.5176	1.01	1.5353
4	.90	--	--	--
5	.11	.7542	.770	.8033
6	.83	.4670	.965	1.6427
7	.90	.4355	.968	1.7489
8	.62	.5763	.519	.7086
9	.34	.7819	1.563	1.5728
11	.14	.8006	1.492	1.4663
12	.76	.5063	1.05	1.6318
13	1.7	.1957	.399	1.6041
14	.11	.7542	1.679	1.7516
15	.07	.5821	1.358	1.8355
17	.74	.5112	1.174	1.8070
18	.09	.6549	1.329	1.5966
19	.46	.6753	1.289	1.5018
20	.18	.8223	2.149	2.0562

*(see Figure 22.)

Av. of ϵ at 1048 A = 1.494

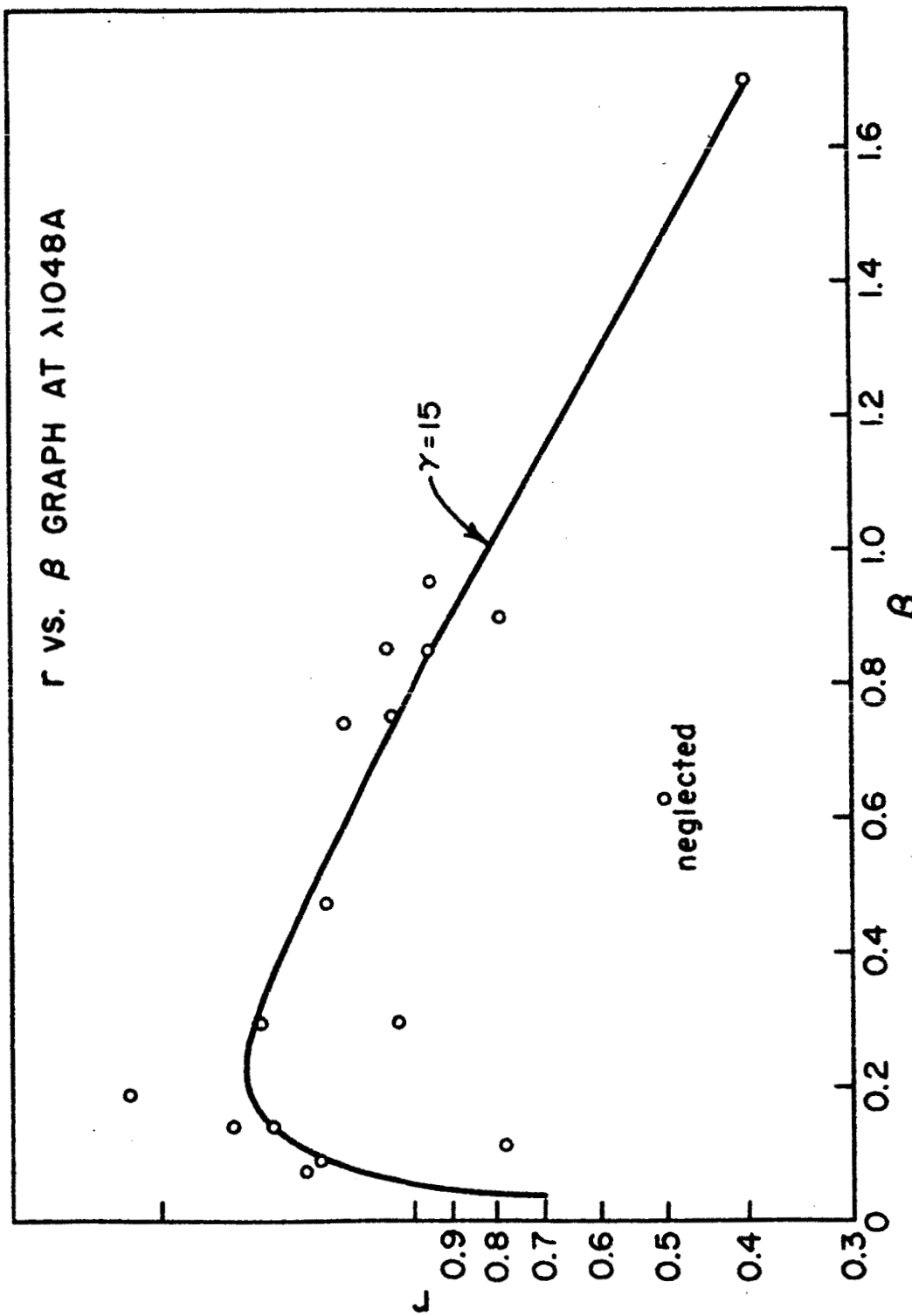
r VS. β GRAPH AT λ1048A
γ=15
neglected
r
β
0.3
0.4
0.5
0.6
0.7
0.8
0.9
0
0.2
0.4
0.6
0.8
1.0
1.2
1.4
1.6

Figure 22

TABLE NUMBER 8.

Summary of data and results.

$F = 1.51$, $\lambda_c = 5461$ Å, $\lambda = 1216$ Å, $*\gamma = 10$

Sample	β	R	r	ϵ
1	.90	.4515	1.004	1.5080
2	.34	.7677	1.50	1.3249
3	.83	.4889	1.00	1.3870
4	.90	--	--	--
5	.11	.6258	1.13	1.2244
6	.83	.4841	1.112	1.5576
7	.90	.4515	1.280	1.9224
8	.62	.5958	1.414	1.6093
9	.34	.7677	1.598	1.4115
11	.14	.6922	1.283	1.2569
12	.76	.5245	1.242	1.6057
13	1.7	.2030	.420	1.4030
14	.11	.6258	1.244	1.3480
15	.07	.4838	.838	1.1745
17	.74	.5294	1.275	1.6331
18	.09	.5640	1.597	1.9201
19	.46	.6903	1.30	1.2770
20	.18	.7438	?	--

*(see Figure 23.)

Av. of ϵ at 1216 A = 1.473

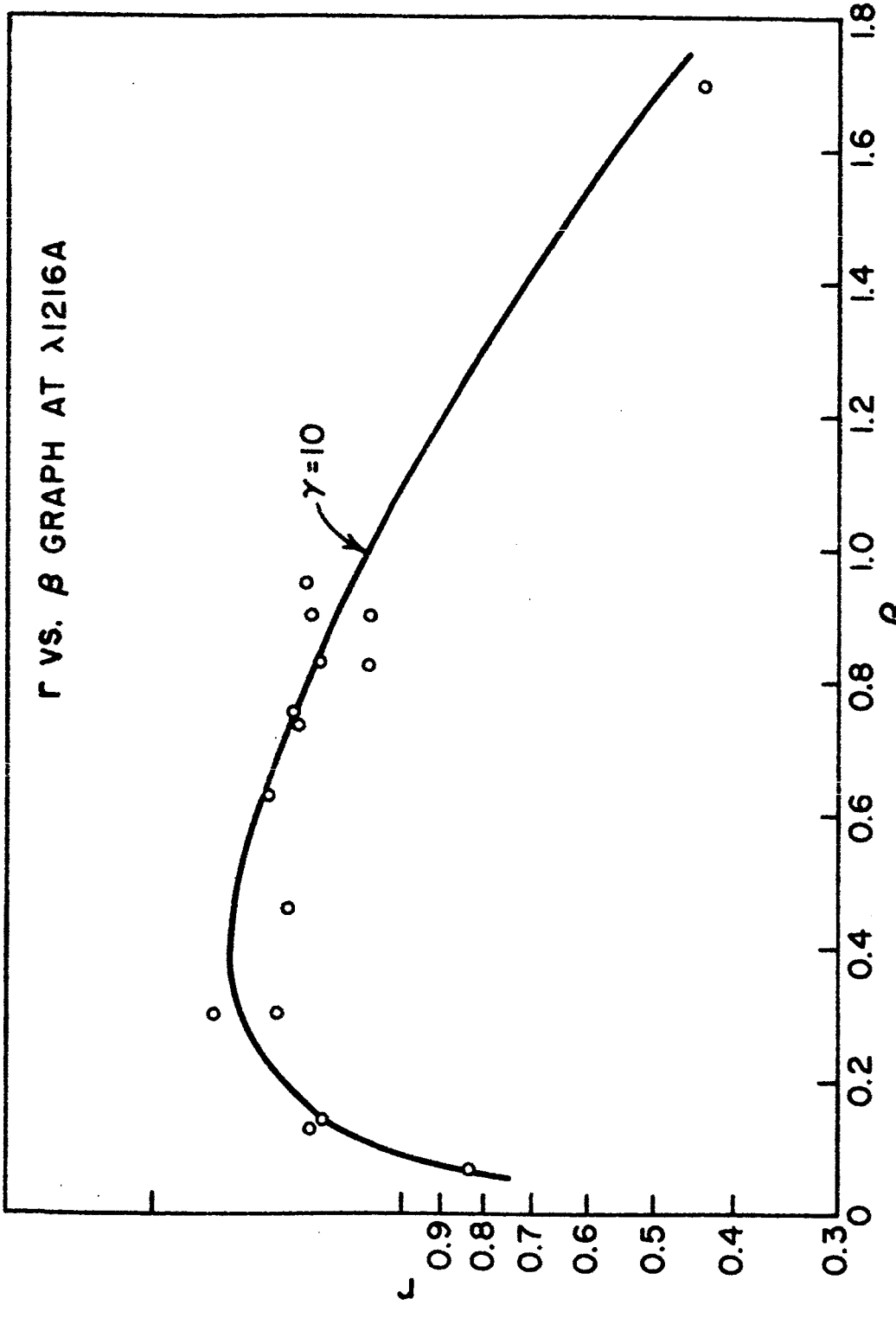
Γ VS. β GRAPH AT λ1216A
γ=10
Γ
β
0.3
0.4
0.5
0.6
0.7
0.8
0.9
0
0.2
0.4
0.6
0.8
1.0
1.2
1.4
1.6
1.8

Figure 23

CHAPTER IV

CONCLUSION

The theory relating the relative luminescence yield of a thin screen and areal density of the screen is in satisfactory agreement with the experimental observations. The equation for the response function in terms of dimensionless parameters is particularly convenient for calculations and should be applicable to a wide variety of phosphors.

The inferences which may be drawn from the results of this experiment stem from two facts about the phosphor $CaWO_4$:Pb which appear out of the present analysis; namely, the absolute quantum efficiency is greater than unity between 304 A and 1216 A, and the absolute quantum efficiency decreases with increasing wavelength with a trend toward reaching a constant value at wavelengths greater than 1000 A. The value of the absolute quantum efficiency of $CaWO_4$:Pb was found to be 4.95 at 304 A, 3.53 at 461 A, 3.02 at 584 A, 1.49 at 1048 A and 1.47 at 1216 A.

There has been no confirmed report of the photoconductivity in a tungstate phosphor[34] between 2200 A and 4000 A. It has been generally assumed that absorption of the UV radiation, at least in the region of the first lattice absorption bands, produces only excitation of the WO_4^{-2} ion and that free electrons are not formed. However, Randalls and Wilkins[35] have shown that this compound is slightly photoconducting while fluorescing. The experimenters claim that this property is certainly not due to chance impurity. The similarity of the emission spectra of various tungstates[34] strongly suggests that the WO_4^{-2} ion is the luminescent center. The work of Dr. Conklin[12] gives added support to this viewpoint. The fact that the ionization potential of the WO_4^{-2} ion group is about 5.6 eV (2200 A), strongly suggests that all the UV photons between 304 A and 1216 A will be effective in the production of secondary photoelectrons, which, in turn, are responsible for the fact that the absolute quantum efficiency is greater than unity.

Lead is an activator for the phosphorescence of calcium and strontium tungstates only if it is present in the proper concentration.[9] In the present experiment lead was 0.7% by weight of $CaWO_4$. With such a small

concentration of lead, $CaWO_4$ centers would surely dominate. Apparently the only function of lead is to increase the absorption wavelength and the peak emission wavelength. This can be seen as a slight change in the shape and positions of the potential energy curve representing the first excited state, corresponding to a slight distortion of the lattice by the lead ions.[12,36]

Among the factors that determine whether a solid shows photoluminescence or not, the state of crystallization is of primary importance. Kroger[16] shows that calcium tungstate, when made by precipitation from a solution, is obtained in the form of small, womewhat imperfect crystals which are practically non-luminescent but which acquire luminescence upon changing their character by further alterations produced primarily by, heat treatments. He has further shown that dissipation of the absorbed energy in tungstate phosphors generally increases at higher temperatures. It is quite likely that the presence of an optimum amount of lead may not only help the crystallization process of calcium tungstate but also may modify the energy levels as to increase the efficiency of emission.

Another possibility is that the powerful 304 A photon may knock out an electron from the WO_4^{-2} group and this photoelectron may transfer its energy to excite the lead atom and give rise to luminescence. Thus $CaWO_4$:Pb may behave partly as a photoconducting and partly as a non-photoconducting phosphor.

The latter possibility is not completely ruled out in view of Botden's paper[17] where it is assumed that the place of absorption and place of emission are differently located within the phosphor. The transfer process (a sort of collision of the second kind, as in gases) is based upon quantum mechanical resonance of the excited state of the primary excited atom with that of another atom (whether of the same kind or not). A quantum mechnaical theory by Kallmann and London[37] indicated that even the optically forbidden transitions may well occur through resonance processes. Also, the observed distances of more than 100 A over which transfer can take place are made plausible. It is very likely that the behavior of lead in certain optimum amounts in $CaWO_4$ may be responsible for this type of quantum mechanical resonance as described above, and it may act as a via-medium between the places of absorption and emission of energy in the

phosphor. The photoconductivity measurements would clarify many details as to phosphor behavior under high energy excitation.

The present investigations have been done at a constant temperature. A very important aspect of phosphor research which has been ignored here is the dependance of luminescence phenomena on temperature. Even at dry ice temperature, effects of interest may appear, and if the phosphor could be cooled down to liquid hydrogen temperature and then gradually warmed up while being excited in the vacuum ultraviolet, a great deal of information might be revealed about effects such as trapping and quenching.

Although wartime developments led to considerable work on the stimulation and quenching of phosphors by infrared, few attempts have actually been made to study the infrared emission. If this could be done, one might understand better the nature of processes which so far are simply called "radiationless" for all practical purposes.

Another completely untouched field of research is the measurements of the absolute quantum efficiency of organic phosphors excited by the extreme UV photons. The mechanisms and theory here are completely different from those of crystal phosphors. One such organic compound is 2,2' dihydroxy 1,1' napthalazine (leumogen) which has constant quantum efficiency between 4600 A and 900 A.[10] Kristianpoller has used this leumogen in the form of a thick slice to measure the absolute quantum efficiency of sodium salycylate.[10]

The discovery of a phosphor which has a very constant absolute quantum efficiency regardless of the wavelength of the impinging radiation, can be successfully used for absolute calibration of unknown ultraviolet radiations. This is important for the present research in the field of rocket solar ultraviolet physics and likewise in the study of the spectrum of stars. A calibrated phosphor can replace the less sensitive thermopile for ultraviolet intensity measurements. The procedure involved in such a calibration is similar to that employed in this work for finding the absolute quantum efficiency, ϵ. The difference is that in equation (4-24), ϵ is to be regarded as a known quantity, and R, the response function as the unknown. After R is found, J_0, the intensity of the UV exciting radiation can be found from equation (4-8).

BIBLIOGRAPHY

1. Harvey, E. Newton, "A History of Luminescence," American Philosophical Society, N. Y.

2. Watanabe, K. and C. Y. Inn, "Intensity Measurements in Vacuum UV," J.O.S.A., 43, 1, p. 32 (January 1953).

3. Thurnau, D. H., "Quantum Efficiency Measurements on Several Phosphors Under Excitation in the Extreme UV," J.O.S.A., 46, 5, p. 346 (May 1956); also his Ph. D. thesis, University of Colorado, Boulder, Colorado (USA), (1957).

4. Samson, "Absolute Intensity Measurements in Vacuum UV," J.O.S.A., 54, 1, p. 6, (January 1964).

5. Seya and Masuda, "On the Relation Between Thickness of Sodium-salicylate and its Response to Extreme UV Light," Science of Light, 12, 1, p. 9, (1963).

6. Bruner, Elmo C. Jr., "The Absolute Quantum Efficiency of Sodium Salicylate Excited by Extreme Ultraviolet Light," Ph. D. thesis, University of Colorado, Boulder, Colorado. Scientific Report, NASA Contract NASr-86 and Air Force contract AF19(628)-287. (June 1964).

7. Knapp and Smith, "Fatigue Effect in Luminescence Yield of Sodium Salicylate," Ap. Opt., 3, 5, p. 637 (May 1964).

8. Taylor, Norman, Thesis, University of Colorado, Department of Physics, Boulder, Colorado. "Absolute Quantum Efficiency of Calcium Tungstate," (1964).

9. Swidells, F. E., "The Luminescence of Alkaline Earth Tungstates Containing Lead," J.O.S.A., 23, 1, p. 129, (April 1933).

10. Kritianpoller, N., and David Dutton, "Optical Properties of Leumogen - a Phosphor for Wavelength Conversion," Ap. Opt. 3, 2, p. 287 (February 1964): Also, "Absolute Quantum Yield of Sodium Salicylate," J. O. S. A., 54, 10, p. 1285, (October 1964).

11. Drusshel, Sommers and Cox, "Correction of Luminescence Spectra and Calculation of Quantum Efficiency Using Computer Techniques," Annalyt. Chem., 35, 13, p. 2166 (December 1963).

12. Conklin, R. L., "The Behavior of Several Phosphors Upon Irradiation in the Vacuum Ultraviolet," Ph. D. thesis, University of Colorado, Physics Department, Boulder, Colorado (1957).

13. Leverenz, H. W., "An Introduction to Luminescence of Solids," John Wiley & Sons, Inc., New York (1950).

14. Pringsheim, P., "Fluorescence and Phosphorescence," Inter-science Publishers, Inc., New York, (1959).

15. Kallmann & Sprutch, Editors, "Luninescence of Organic and Inorganic Materials," papers presented at the International Conference on Luminescence, New York (1961), John Wiley & Sons, Inc. N. Y. (1962).

16. Kroger, F. A., "The Temperature Dependence of the Fluorescence of Tungstate and Molybdate in Relation to the Perfection of the Lattice," Phillips Research Report, 2, p. 340-348 (1947).

17. Botden, P. J. "Transfer and Transport of Energy by Resonance Processes in Luminescent Solids," Phillips Research Report, 6, p. 425-473 (1951).

18. Kittel, C., "Introduction to Solid State Physics," John Wiley & Sons, Inc., New York (1953).

19. Deckker, A. J., "Solid State Physics," Prentice Hall, Inc., N. J. (1954).

20. Kittel, C., "Introduction to Solid State Physics," p. 296, John Wiley & Sons, Inc., N. Y. (1953).

21. Kip & Kittel, "Cyclotron Resonance of Electrons and Holes in Silicon & Germanium Crystals," Phys. Rev., 98, p. 368 (1955).

22. Klasens, H. A., "Transfer of Energy Between Centers in Zinc Sulphide Phosphors," Nature, 158, p. 306, (1946).

23. Klasens, H. A. and Ramson & Quantic, "The Relation Between Efficiency and Exciting Intensity for Zinc Sulphide Phosphor," J.O.S.A., 38, p. 60 (1948).

24. Lambe and Klick, "Model for Luminescence and Photoconductivity in the Sulphides," Phys. Rev. 98, p. 909 (1955).

25. Larach and Turkevitch, "Magnetic Properties of Zinc Sulphide and Cadmium Sulphide Phoshors," Phys. Rev., 98, p. 1015, (1955).

26. Williams, F. E., "Advances in Electronics," 5, p. 137, (1953).

27. Leverenz, (as in reference 13) p. 130.

28. Newburgh, Heroux and Hinteregger, "Two Light Sources for Use in the Extreme UV," App. Opt. 1, p. 733 (1962).

29. Jenkins and White, "Fundamentals of Optics," McGraw Hill Book Company, New York (1950) p. 198.

30. Savine, "Reflectivities of Evaporated Metal Films in Near and Far UV," Phys. Rev., 55, p. 1064 (1939).

31. Walker, Rustgi and Weissler, "Optical and Photoelectric Properties of Thin Metallic Films in Vacuum UV," J.O.S.A., 49, p. 471 (1959).

32. Brown, Chasmar and Fellget, "The Construction of Radiation Thermopile Using Semi-conducting Thermoelectric Materials," J. Sci. Inst. 30, p. 195 (1953).

33. Fowler, Rense and Simmons, "Film Calibration for Rocket UV Spectrographs," App. Opt. 4, p. 1596, (December 1965).

34. Klick and Schulmann, "Absence of Photoconductivity in Tungstate Phosphors," Phys. Rev., 75, p. 1606 (1949).

35. Randalls and Wilkins, "The Phosphorescence of Various Solids," Proc. of Roy. Soc. A., 184, p. 346, (1945).

36. Hameka and Vlam, "The Luminescence Spectrum of Calcium Tungstate According to the Configuration Coordinate Model," Physica, 19, p. 943 (1953).

37. Kalmann and London, Z. phys. Chemie B2, 207-243 (1929).

APPENDIX A.

Tables of Response Function R (β, γ)

$$R(\beta, \gamma) = \frac{\gamma}{\gamma-1}\left[e^{-\beta} - e^{-\gamma\beta}\right]$$

β	R(β,1)	R(β,4)	R(β,6)	R(β,10)
.00	.0000	.0000	.0000	.0000
.02	.0196	.0761	.1120	.1794
.04	.0384	.1449	.2040	.3224
.06	.0565	.2069	.2929	.4367
.07	.0653	.2355	.3305	.4842
.09	.0822	.2882	.3974	.5637
.10	.0905	.3126	.4272	.5965
.15	.1291	.4158	.5449	.7084
.20	.1637	.4925	.6210	.7593
.30	.2222	.5861	.6906	.7678
.40	.2681	.6245	.6955	.7244
.50	.3032	.6282	.6680	.6664
.80	.3594	.5456	.5293	.4988
.90	.3659	.5057	.4825	.4517
1.0	.3679	.4661	.4385	.4080
1.2	.3614	.3906	.3606	.3347
1.4	.3452	.3238	.2957	.2740
1.6	.3230	.2669	.2422	.2243
1.8	.2975	.2195	.1984	.1837
2.0	.2706	.1800	.1624	.1503

APPENDIX A (continued).

β	R(β, 15)	R(β, 20)	R(β, 30)	R(β, ∞)
.00	.0000	.0000	.0000	1.0000
.02	.2565	.3262	.4463	.9802
.04	.4415	.5384	.6824	.9610
.06	.5735	.6743	.8033	.9417
.07	.6242	.7219	.8379	.9326
.09	.7016	.7880	.8759	.9139
.10	.7305	.8100	.8845	.9051
.15	.8094	.8536	.8789	.8608
.20	.8240	.8425	.8444	.8187
.30	.7819	.7771	.7662	.7408
.40	.7156	.7052	.6934	.6704
.50	.6493	.6384	.6274	.6066
.80	.4815	.4729	.4648	.4493
.90	.4357	.4280	.4206	.4065
1.0	.3942	.3872	.3806	.3679
1.2	.3228	.3170	.3116	.3014
1.4	.2642	.2596	.2551	.2466
1.6		.2125		.2018
1.8		.1740		.1653
2.0		.1424		.1353